Technical Report Documentation Page

1. Report No.	2. Government Accession No.	3. Recipient's Catalog No.
FHWA/TX-92+1169-4		

4. Title and Subtitle	5. Report Date
TERMINAL MOVEMENT IN CONTINUOUSLY REINFORCED CONCRETE PAVEMENTS	January 1992
	6. Performing Organization Code
7. Author(s)	8. Performing Organization Report No.
Wan-Yi Wu and B. Frank McCullough	Research Report 1169-4
9. Performing Organization Name and Address	10. Work Unit No. (TRAIS)
Center for Transportation Research The University of Texas at Austin Austin, Texas 78712-1075	11. Contract or Grant No. Research Study 3-8-88/1-1169
	13. Type of Report and Period Covered
12. Sponsoring Agency Name and Address Texas Department of Transportation Transportation Planning Division P. O. Box 5051 Austin, Texas 78763-5051	Interim
	14. Sponsoring Agency Code

15. Supplementary Notes

Study conducted in cooperation with the U. S. Department of Transportation, Federal Highway Administration

Research Study Title: "Concrete Pavement Design Update"

16. Abstract

The purpose of this study is to provide pavement designers with substantive information about CRCP terminal movement. A mechanistic model, PSCP2, was used to analyze free end movement and to predict the size of terminal movements. Field measurements were conducted at SH225 in Houston, Texas, in order to supplement the CRCP movement field data obtained from a previous research study. A comparison between the collected data and the predictions of the PSCP2 program was performed to verify the reliability of the PSCP2 mechanistic model. A procedure was then developed that estimates the terminal movement of a CRC pavement.

17. Key Words	18. Distribution Statement
CRCP terminal movement, mechanistic model, PSCP2, free end movement, field measurements, data, predictions, reliability, pavement design	No restrictions. This document is available to the public through the National Technical Information Service, Springfield, Virginia 22161.

19. Security Classif. (of this report)	20. Security Classif. (of this page)	21. No. of Pages	22. Price
Unclassified	Unclassified	54	

TERMINAL MOVEMENT IN CONTINUOUSLY REINFORCED CONCRETE PAVEMENTS

by

Wan-Yi Wu
B. Frank McCullough

Research Report Number 1169-4

Research Project 3-8-88/1-1169
Concrete Pavement Design Update

conducted for

Texas Department of Transportation

in cooperation with the

U.S. Department of Transportation
Federal Highway Administration

by the

CENTER FOR TRANSPORTATION RESEARCH
Bureau of Engineering Research
THE UNIVERSITY OF TEXAS AT AUSTIN

January 1992

NOT INTENDED FOR CONSTRUCTION,
PERMIT, OR BIDDING PURPOSES

W. Ronald Hudson, P.E. (Texas No. 16821)
B. Frank McCullough, P.E. (Texas No. 19914)
Research Supervisors

PREFACE

This report is part of Research Project 3-8-88/1-1169, "Concrete Pavement Design Update." This study was conducted by the Center for Transportation Research, Bureau of Engineering Research, The University of Texas at Austin. This study was sponsored by the Texas Department of Transportation and the Federal Highway Administration under an agreement with The University of Texas at Austin and the Texas Department of Transportation.

The authors wish to express their appreciation to all project staff and to the rest of the Center for Transportation Research personnel for their assistance and invaluable contributions. The authors also want to thank Mr. David Whitney and Mr. Charles Boatner, who assisted with the field measurements. The Texas Department of Transportation personnel, in particular Mr. James Brown and Mr. Andrew Wimsatt, were always helpful and always generous with their time.

ABSTRACT

The purpose of this study is to provide pavement designers with substantive information about CRCP terminal movement. A mechanistic model, PSCP2, was used to analyze free end movement and to predict the size of terminal movements. Field measurements were conducted at SH 225 in Houston, Texas, in order to supplement the CRCP movement field data obtained from a previous research study. A comparison between the collected data and the predictions of the PSCP2 program was performed to verify the reliability of the PSCP2 mechanistic model. A procedure was then developed that estimates the terminal movement of a CRC pavement.

SUMMARY

This report analyzes the terminal movement characteristics of CRCP using PSCP2, a mechanistic model developed by the Center for Transportation Research (CTR). The study demonstrates that the factors affecting terminal movement are temperature change, slab length, slab thickness, aggregate type, season of placement, and friction force. Field measurements of free end movements on a CRCP were performed on SH 225 in Houston, Texas. Both longitudinal and transverse movements were measured, with the results used to supplement the terminal movement field data obtained from a previous research study. In order to verify the reliability of the PSCP2 program, the program's predictions were compared with the field data. It was determined from the comparison that the PSCP2 program could effectively predict the terminal movement if the input was correct. Finally, a procedure was developed to enable a pavement designer to quantify the end movement at a specific site on a project.

IMPLEMENTATION STATEMENT

The type of terminal treatment used for CRCP is dependent on the magnitude of movement expected at a particular project site. Yet, as this study demonstrates, actual end movements are themselves dependent on a site's particular annual temperature range, subbase type, pavement thickness, and season in which the pavement is to be placed. Consequently, a treatment found to be successful at one location may prove to be inadequate at another.

The designer in such cases must estimate the anticipated movements on the project. Equation 5.4 in this report provides a method for reliably estimating such site-specific movement. The procedure, requiring indirect tensile tests on the subbase material of interest, along with other site-specific information, thus allows the designer to identify the most appropriate terminal treatment.

TABLE OF CONTENTS

PREFACE ..... *iii*

ABSTRACT ..... *iii*

SUMMARY ..... *iii*

IMPLEMENTATION STATEMENT ..... *iv*

CHAPTER 1. INTRODUCTION

1.1 GENERAL COMMENTS *1*
1.2 OBJECTIVES OF THE STUDY *1*
1.3 SCOPE *1*

CHAPTER 2. DATA ANALYSIS USING MECHANISTIC MODELING

2.1 BACKGROUND *3*
2.2 THE ANALYSIS PROGRAM *3*
2.3 INPUT DATA AND VARIABLES *4*
2.3.1 Concrete Property Inputs *4*
2.3.1.1 Thermal Coefficient *4*
2.3.1.2 Compressive Strength *4*
2.3.1.3 Other Concrete Properties *5*
2.3.2 Coefficient of Friction-Displacement Relationship *5*
2.3.3 Stiffness of Slab Support *6*
2.3.4 Steel Properties *6*
2.3.5 Environmental Inputs *6*
2.3.5.1 Temperature Data for Initial Period *6*
2.3.5.2 Temperature Data for the Subsequent Period *6*
2.4 ANALYSIS FACTORIAL *6*
2.5 ANALYSIS RESULTS *7*
2.5.1 End Movement and Slab Length *7*
2.5.1.1 General Concept *7*
2.5.1.2 Aggregate Type *9*
2.5.1.3 Subbase Friction Force *10*
2.5.1.4 Placement Season *11*
2.5.1.5 Slab Thickness *11*
2.5.1.6 Summary *12*
2.5.2 End Movement in Relation to Slab Temperature *12*
2.5.2.1 General Concept *12*
2.5.2.2 Summary *13*

CHAPTER 3. ANALYSIS USING FIELD DATA

3.1 BACKGROUND 14
3.2 FIELD INSTRUMENTATION AND DATA COLLECTION 14
3.2.1 Description of Measurement Section 14
3.2.2 Selection of Measurement Locations 15
3.2.3 Description of the Instrument 15
3.2.4 Selection of Measurement Time 18
3.3 DATA PRESENTATION 19
3.4 DATA ANALYSIS 19
3.4.1 Statistical Analysis 19
3.4.2 Transverse Movement 20
3.4.3 End Movement 21
3.4.4 Summary 21

CHAPTER 4. COMPARISON OF MECHANISTIC RESULTS WITH FIELD DATA

4.1 BACKGROUND 22
4.2 DESCRIPTION OF COMPARED DATA 22
4.2.1 Field Data 22
4.2.1.1 SH 225 in Houston 22
4.2.1.2 Research Project 39 23
4.2.2 Predicted Data 23
4.3 RESULTS OF COMPARISON 24
4.4 CALIBRATION 24
4.5 SUMMARY 25

CHAPTER 5. IMPLEMENTATION

5.1 INTRODUCTION 26
5.2 DEVELOPMENT OF DESIGN EQUATION 26
5.3 IMPLEMENTATION OF THE MECHANISTIC PSCP2 MODEL 27
5.3.1 Overview Evaluation Procedure 28
5.3.2 Project Evaluation Procedure 28

CHAPTER 6. CONCLUSIONS AND RECOMMENDATIONS

6.1 CONCLUSIONS 29
6.2 RECOMMENDATIONS FOR PREDICTING END MOVEMENT 29
6.3 RECOMMENDATIONS FOR FUTURE STUDY 30

REFERENCES 31

APPENDIX A. GRAPHS OF END AND SEASONAL MOVEMENT IN RELATION TO SLAB LENGTH 33

APPENDIX B. GRAPHS OF RATE OF MOVEMENT IN RELATION TO SLAB LENGTH 41

APPENDIX C. DATA FROM MEASUREMENT TAKEN ON SH 225 IN HOUSTON 46

APPENDIX D. GRAPHS OF GAUGE PLUG READINGS AND SLAB TEMPERATURES AT SH 225 IN HOUSTON 47

CHAPTER 1. INTRODUCTION

1.1 GENERAL COMMENTS

Volume change is a significant consideration in the design of continuously reinforced concrete pavement (CRCP) structures. If the length of a pavement is substantial, volume changes related to thickness and width can be overlooked (Ref 2). But changes in pavement length—referred to as longitudinal movement—represent the more serious problem: excessive longitudinal movement, whether it involves expansion or contraction, can be detrimental to the pavement's structural integrity. For example, if expansion occurs unchecked, an adjacent pavement section or the adjacent abutment walls of a bridge may be damaged. In addition, excessive contraction can impair the load transfer at the joints and can reduce the ride quality of the pavement.

Since CRCP is essentially a long slab without joints (other than construction joints), the pavement designer must especially consider longitudinal movement occurring at the end portions of the slab. After first identifying the significant factors affecting CRCP end movements, the designer then selects the most suitable technique for absorbing or reducing CRCP end movement.

In previous studies (Refs 2 through 5), the factors influencing the free end movement of CRCP have been evaluated by analyzing the terminal movements data obtained from in-service pavements. These factors include environmental conditions, slab geometry, and the coefficient of friction between the pavement and the subbase.

In this study, we first reviewed the literature on design or construction methods that accommodate or restrict terminal movement for CRCP. Among the several methods identified, we particularly noted the use of expansion joints, steel finger joints, and wide-flange beam joints (Refs 5, 6, 8, and 13) to accommodate longitudinal movement (a space is created so that the longitudinal movement is allowed). We also found references to the end anchorage system, in which a series of concrete lugs are extended beneath the slab. While this system can be used in many cases to restrain pavement movement, it cannot be used where soil characteristics prove inadequate—that is, where the soil's displacement resistance is marginal (Ref 8).

Information on terminal movement based on observations of existing CRCP's proved more limited. Consequently, in this report we argue that a mechanistic computer model capable of predicting the end movement for a range of conditions represents the best way to fully understand the end movement of CRCP. After the analyst calibrates the movements predicted by the mechanistic computer program using the observed performance of pavement in the field, the mechanistic model can accurately predict the end movement. The designer can then use these predictions to choose the most suitable techniques that will accommodate the effects of the terminal movement.

1.2 OBJECTIVES OF THE STUDY

The general objective of this study is to provide substantive information that will help the designer predict CRCP terminal movement. Within this framework, we identified the following specific objectives:

(1) to determine the terminal movement characteristics of CRCP using a mechanistic model and to verify those characteristics with field data;
(2) to conduct a sensitivity study of the problem; and
(3) to develop charts that may be used by designers to estimate movements for a range of conditions.

1.3 SCOPE

Because an examination of all possible considerations would have required an extensive study, we narrowed the scope of this investigation to an analytical study of CRCP only, with the report then limited to developing design information. The scope can be summarized as follows:

(1) The focus is on the free end movement of CRCP without traffic (i.e., terminal anchorages and effects of traffic are not considered).
(2) The mechanistic model, PSCP2, is used to analyze the terminal movement.
(3) The data from a previous project and selected case studies are used for verification.

The outline of the report is as follows:

Chapter 2 describes the selection of the PSCP2 program, which analyzes terminal movements. The PSCP2 program, its input requirement, the analysis design factorial, and the analysis of results are presented.

Chapter 3 includes the field measurements of slab movements. The test section developed for verification purposes and the instrumentation for field measurements are described. The data collected in the measurements are analyzed and discussed.

Chapter 4 compares the collected data against the predictions of the PSCP2 program. The calibrated results of subbase friction are presented.

Chapter 5 describes the implementation of the PSCP2 mechanistic model, and the design equation and design charts are developed for pavement designers to estimate the terminal movement in CRCP's.

Finally, Chapter 6 contains the conclusions and the recommendations drawn from this study.

CHAPTER 2. DATA ANALYSIS USING MECHANISTIC MODELING

2.1 BACKGROUND

The terminal movement of concrete pavements has long been studied by analyzing the observed performance of in-service pavements. But because these in-service pavement data are limited, the number of cases that can be considered (and hence yield reliable results) is limited as well. Thus, conditions and effects frequently are investigated by empirical extrapolation only. And while researchers are for the most part aware of the primary factors that affect terminal movement, they do not fully understand the effects of terminal movements in all circumstances. Such an understanding would facilitate and improve the design of terminal anchorages.

Many computer models can simulate the behavior of concrete pavements. One particular model, the program PSCP2, can be used specifically to predict the movement of concrete pavement. Using PSCP2, researchers can study—through computational techniques—the effects of terminal movements for various conditions.

This chapter analyzes terminal movements under different combinations of variables using the PSCP2 program. It describes the PSCP2 program, its input requirement, the analysis design factorial, and the analysis results.

2.2 THE ANALYSIS PROGRAM

The data analysis of this report was performed using the PSCP2 computer program (Ref 11) developed by the Center for Transportation Research of The University of Texas at Austin. The PSCP2 program, providing as it does a complete analytical procedure for prestressed concrete pavement, is especially useful in predicting movement in a long pavement. This capability is not present in other programs. For example, the JRCP mechanistic computer program can give a researcher joint width information that can be used to predict slab movement (Ref 14); however, the input of the slab length is limited. When the length of the slab exceeds a certain value, the JRCP program does not produce viable results (Ref 15). Furthermore, the JRCP model does not account for the condition of full sliding present in longer pavements.

The PSCP2 program has another important advantage: the slab movement prediction capability of the program has an input requirement that allows the researcher to select the time of year at which the slab movement should be predicted. Thus, different seasons of observation can be chosen that are consistent with the parameters of the study.

The following assumptions are intrinsic to the application of the PSCP2 program model (Refs 11 and 12):

(1) Concrete is a homogeneous, linearly elastic material. The slab is a solid body having no discontinuities (e.g., cracks).
(2) The frictional resistance produced by dowels, tie bars, and lanes adjacent to the longitudinal movements of the slab is disregarded.
(3) The friction coefficient versus displacement relationship that characterizes the frictional resistance under the slab is represented in Figure 2.1.
(4) The temperature variations considered in this analysis are those that occur at the slab's middepth. Additionally, the friction stresses that develop will be evenly distributed on the cross section—an assumption that makes applicable a one-dimensional analysis of an axial structural member.
(5) The redistribution of the slab weight, owing to curling and warping, that affects the friction forces developing beneath the slab is disregarded.
(6) The effect of concrete creep before the application of prestress forces is also disregarded.
(7) Symmetry of conditions with respect to the geometric center of the slabs is assumed. Therefore, the analysis is limited to a half-slab length, with the geometric center being fixed.

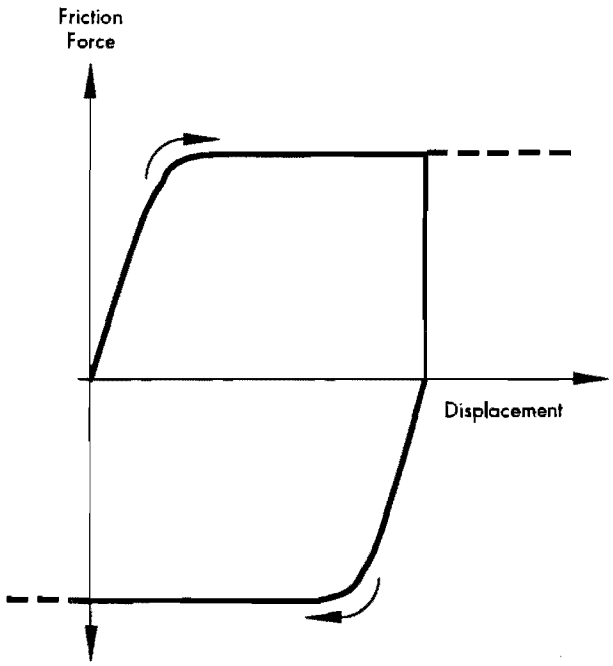

Figure 2.1 Friction force versus displacement curve assumption for the PSCP2 mechanistic computer program (Ref 11)

(8) The origin for slab length X in the longitudinal direction is at the mid-slab. Friction forces are positive in the positive X direction. Movements in the positive X direction are also positive. Friction forces and movements are always of opposite signs. Tensile stresses in the concrete are positive. Mid-depth temperature changes are positive if these changes represent temperature increments of a given time in comparison with an earlier time considered.

(9) The vertical reaction, Yk, to any section is directly proportional to the deflection, Y, with the proportionality constant k being the modulus of subgrade reaction.

(10) Zero deflection is at the rest position on the subgrade level of the initial deflection.

Since the functions and the assumptions outlined above apply favorably to CRCP, we selected the PSCP2 mechanistic computer program as the analysis model.

2.3 INPUT DATA AND VARIABLES

The variables considered in this study for input into the PSCP2 program are aggregate type, friction force, slab thickness, and season of placement.

2.3.1 Concrete Property Inputs

Research Report 422-2, "Design Recommendations for Steel Reinforcement of CRCP" (Ref 7), showed that siliceous river gravel (SRG) and limestone (LS) aggregates, when used exclusively, yield concrete mixes whose material properties differ significantly. Since these two aggregate types are widely used in Texas, they are the principal aggregates considered in this study. The concrete property inputs, such as thermal coefficient and compressive strength, were given two values: one value for SRG and one value for LS. Other concrete property inputs, such as the ultimate shrinkage strain, the unit weight, the Poisson ratio, and the creep coefficient, are treated as constant values for each item.

2.3.1.1 Thermal Coefficient

Table 2.1 shows the thermal coefficient values (by aggregate type) used for the PSCP2 program input (Ref 7).

Table 2.1 Inputs of thermal coefficient (Ref 7)

Coarse Aggregate Type	Thermal Coefficient
SRG	8×10^{-6} in./in./°F
LS	6×10^{-6} in./in./°F

2.3.1.2 Compressive Strength

In the PSCP2 program, if the value of the 28th day compressive strength is given, the relationship between compressive strength and pavement age will be derived from that value given by the program. Table 2.2 lists, by coarse aggregate type, the 28th day compressive strength input. The input curves of compressive strength developed by the PSCP2 program are shown in Figure 2.2.

Table 2.2 The 28th day compressive strength

Coarse Aggregate Type	28th Day Compressive Strength (psi) (Ref 7)
SRG	4,000
LS	5,000

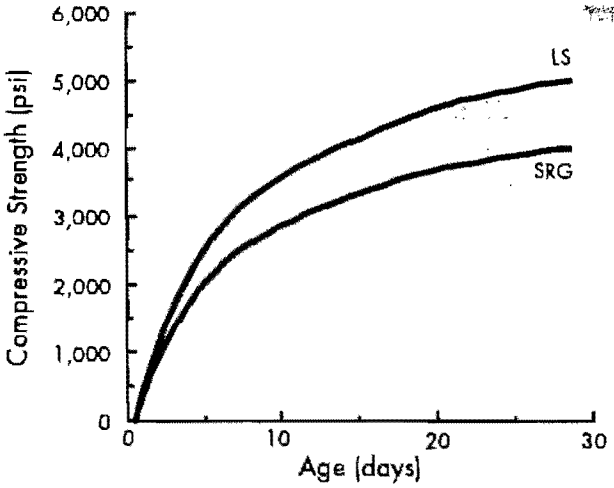

Figure 2.2 Compressive strength input curves for concrete with limestone and with siliceous river gravel aggregates

2.3.1.3 Other Concrete Properties

The concrete properties listed in Table 2.3 were treated as constant values to be input into the PSCP2 program. It should be noted that the input value of the ultimate shrinkage strain for the PSCP2 program was given as zero, since the primary purpose of this study was to predict the daily and annual changes of end movement *after the first year*. The basic approach was to compute the annual movements after the slab movement stabilizes, i.e., after total concrete shrinkage has occurred. The other values listed in the table were based on the characteristics of a typical concrete slab.

Table 2.3 Concrete property inputs (Ref 11)

Concrete Property	Value
Ultimate shrinkage strain	0
Unit weight	144 pcf
Poisson ratio	0.2
Creep coefficient	2.1

2.3.2 Coefficient of Friction-Displacement Relationship

In Research Report 459-2F, "Methods of Analyzing and Factors Influencing Frictional Effects of Subbases," by Andrew W. Wimsatt, et al (Ref 16), the experimental friction forces acting between CRCP and several types of subbases are discussed. Figure 2.3, based on Report 459-2F, illustrates the friction-movement relationship that was used for this study. Figure 2.3 shows that after the curve reaches the maximum friction force, sliding occurs. Before sliding occurs, the curve is in the elastic range of the material beneath the slab. The selected friction forces at sliding levels are 1.0, 4.6, and 15.0 psi. The 1.0 psi is indicative of a subbase with polyethylene sheeting, the 4.6 psi is indicative of an asphaltic subbase, and the 15.0 psi represents CTB (Ref 16).

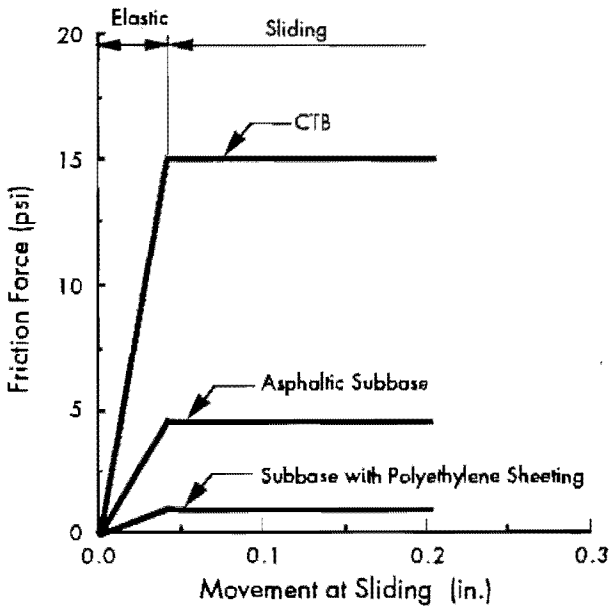

Figure 2.3 Friction-sliding movement input relationships for CTB, asphaltic subbase, and subbase with polyethylene sheeting

Because the PSCP2 program requires a coefficient of friction, the friction forces must be converted to a coefficient of friction. The relationship between friction force and coefficient of friction, assuming that the unit weight of the concrete is 144 pcf, is the following:

$$\mu = \frac{12f}{D}$$

where: μ = coefficient of friction,
f = friction force, psi, and
D = depth of slab, inches.

The inputs for the relative friction values for an 8- and a 12-inch pavement for the PSCP2 program are listed in Table 2.4. They represent the pre-sliding values.

Table 2.4 Inputs of coefficient of friction

Friction Force (psi)	Coefficient of Friction	
	8-in.-Thick Slab	12-in.-Thick Slab
1.0	1.5	1.0
4.6	6.9	4.6
15.0	22.5	15.0

2.3.3 Stiffness of Slab Support

A stiffness of slab support, designated as the K-value, of 500 pci was selected as the input value. This is a typical composite K-value for a stabilized subbase.

2.3.4 Steel Properties

Since the PSCP2 program was designed for prestressed concrete pavement, there are inputs for prestressed steel strands. However, because there is no prestress in CRCP, all of the values of the steel properties for the PSCP2 program were given as zero. Thus, the CRCP was analyzed as a prestressed concrete pavement having no prestress. Cracks in the pavement are, in such an analysis, consequently overlooked in the computer output. In reality CRCP does of course experience cracking, but those cracks occurring in the interior do not affect end movement (Refs 13 and 17).

2.3.5 Environmental Inputs

The PSCP2 program analysis requires pavement temperature data for critical periods throughout the pavement's service life. The pavement temperature data fall into two categories: one is the sequence of temperature for the initial period, i.e., the temperature of the pavement as it hardens; the other is the temperature data for subsequent periods, i.e., the typical daily temperature for the season in which the analysis is taking place. The former category requires that a number of temperature sequences be considered during the initial period, namely, the mid-depth temperature when the concrete sets up (curing temperature), and the mid-depth and top/bottom temperature differentials at each of the temperature sequence periods. The temperature sequence period is set at 2-hour intervals. The latter category requires twelve pairs of mid-depth and top/bottom temperature differentials (for a 24-hour cycle) for the desired data output period.

All the computer program data were obtained from field measurements that were collected during the construction of prestressed concrete near Waco, Texas, and from experimental test sections in Houston, Texas (Refs 18 and 19).

2.3.5.1 Temperature Data for Initial Period

For this study, a range of curing temperatures was obtained by selecting the summer and winter placement periods. The curing temperature forms the basis (or base temperature) by which thermal movements of different time periods are compared. Owing to the two placement seasons, two sets of field data input were collected in the winter and in the summer for the PSCP2 program. Table 2.5 shows the typical curing temperatures used for winter and summer placement (Ref 19).

Table 2.5 Seasonal concrete curing temperatures (Ref 19)

Placement Season	Curing Temperature (°F)
Winter	70
Summer	87

2.3.5.2 Temperature Data for the Subsequent Period

In this study, terminal movement predictions were calculated for the winter, summer, and fall, with the pavement temperature data for those seasons specifically investigated. The ranges of the selected temperatures for each season are shown in Table 2.6 (Ref 18).

Table 2.6 Ranges of seasonal concrete temperature

Observation Season	Mid-depth Temperature of the Concrete (°F)
Winter	36 to 53
Summer	83 to 108
Fall	55 to 79

2.4 ANALYSIS FACTORIAL

The factorial for analysis for the PSCP2 mechanistic computer program is shown in Figure 2.4. As described earlier, the four variables considered form twenty-four sets of combinations. Different slab lengths ranging from 50 to 3,000 feet were tested, with each combination of variables shown in the figure. Thus, a total of 300 computations were made with the PSCP2 mechanistic computer program.

Aggregate Type			SRG		LS	
Slab Thickness (in.)			8	12	8	12
Summer Placement	Friction	1.0	x	x	x	x
		4.6	x	x	x	x
		15.0	x	x	x	x
Winter Placement	Friction	1.0	x	x	x	x
		4.6	x	x	x	x
		15.0	x	x	x	x

Figure 2.4 Analysis factorial

2.5 ANALYSIS RESULTS

The results of the analysis are divided into two parts. The first part investigates the effect of aggregate type, subbase friction force, season of placement, and slab thickness on the relationship between end movement and slab length. The second part studies the effect of end movement in relation to slab temperature.

2.5.1 End Movement and Slab Length

The following sections present a general concept for end movement and slab length. In these discussions, different aggregate types, friction forces, thicknesses, and placement seasons are specifically compared.

2.5.1.1 General Concept

The slab length used in the PSCP2 program is the total length of the slab. Only half of the slab length, however, is contributing to the end movement at one end of the pavement. Figure 2.5 illustrates the relationship between total slab length, L, and total end movement, 2ΔX. Note that the end movement on both ends is one-half of the total end movement, ΔX, which is the result shown by the PSCP2 program.

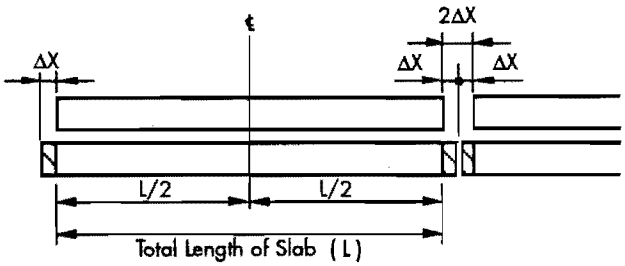

Figure 2.5 The relationship of total slab length and total end movement

In the PSCP2 output for each slab length, there are twelve end movements for each seasonal observation. Every end movement corresponds to one slab temperature that is part of the typical daily temperature cycle (twelve temperatures) for each season. The relationship between end movement and slab temperature is illustrated in Figure 2.6. Generally, when the slab temperature is equal to the curing temperature, the end movement is zero, since there is no temperature change. When the slab temperature is higher than the curing temperature, e.g., during summer observations, positive movement (expansion) is produced. When the slab temperature is lower than the curing temperature, e.g., during winter observations, the end movement is negative (contraction). For instance, Figure 2.6(a) indicates that, for summer placement, the ratio of temperature change between summer and winter

$$\left(\frac{\Delta Tsw}{\Delta Tss}\right)$$

is smaller than the ratio of end movement

$$\left(\frac{\Delta Xsw}{\Delta Xss}\right)$$

since the pavement slides in the winter and remains in the elastic range in the summer. For winter placement, Figure 2.6(b) shows that the ratio of temperature change between summer and winter

$$\left(\frac{\Delta Tww}{\Delta Tws}\right)$$

is approximately equal to the ratio of end movement

$$\left(\frac{\Delta Xww}{\Delta Xws}\right),$$

because the sliding that occurs both in the summer and in the winter is in the elastic range.

The end movement and slab length relationship illustrated in Figure 2.7(a) was obtained by choosing the maximum expansion, ΔXss (see Figure 2.6(a)), and the maximum contraction, ΔXsw, from different slab lengths. In Figure 2.7(a), there are two curves in the plot, one for winter observations and one for summer observations.

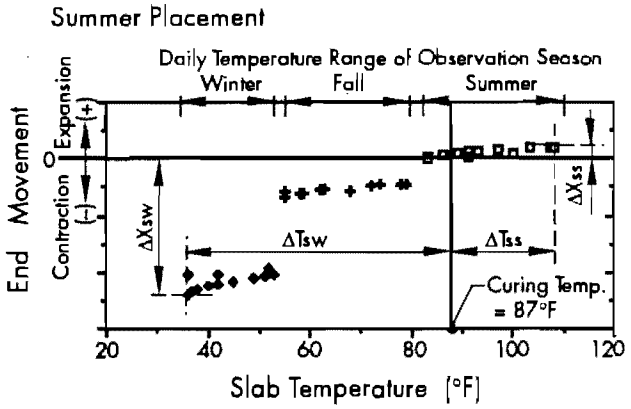

(a) Relationship between end movement and slab temperature for summer placement

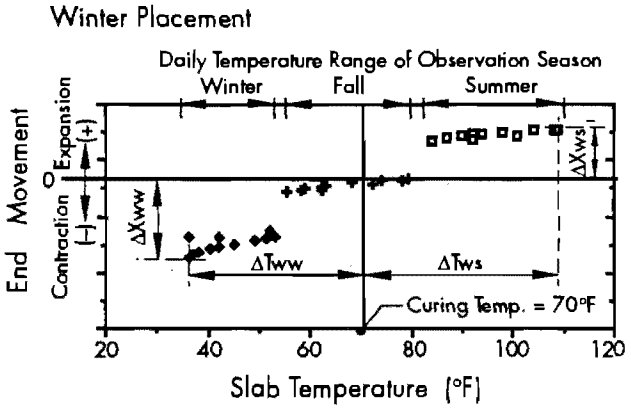

ΔTij = Maximum Temperature Change
ΔXij = Maximum End Movement
i = Placement Season
j = Observation Season
w = Winter
s = Summer

(b) Relationship between end movement and slab temperature for winter placement

SUMMER PLACEMENT:
ΔTsw = Maximum temperature change in a year during which contraction of pavement occurs.
ΔTss = Maximum temperature change in a year during which expansion of pavement occurs.

WINTER PLACEMENT:
ΔTww = Maximum temperature change in a year during which contraction of pavement occurs.
ΔTws = Maximum temperature change in a year during which expansion of pavement occurs.

SUMMER PLACEMENT:
ΔXsw = Maximum contraction of pavement, summer placement.
ΔXss = Maximum expansion of pavement, summer placement.

WINTER PLACEMENT:
ΔXww = Maximum contraction of pavement, winter placement.
ΔXws = Maximum expansion of pavement, winter placement.

Figure 2.6 Relationship between end movement and slab temperature

These curves represent the daily end movements; the summer movements are smaller as a result of slight temperature changes that allowed the end movements to remain in the elastic range (see Figure 2.6(a)). The difference in end movements between these two observations (summer and winter) may be designated as the seasonal movement—that is, the total movement in a year. The plot of the seasonal movement in relation to slab length is shown in Figure 2.7(b). Note that the curve in Figure 2.7(b) tends to become asymptotic and that a "break point" occurs on the graph where longer lengths do not produce greater movement. In other words, when slab length is less than the "break point," the size of the end movement is determined by the slab length. Likewise, when the slab length is greater than the "break point," the end movement is invariably equal to the maximum end movement. The "break point" is defined as the maximum length of slab contributing to the end movement.

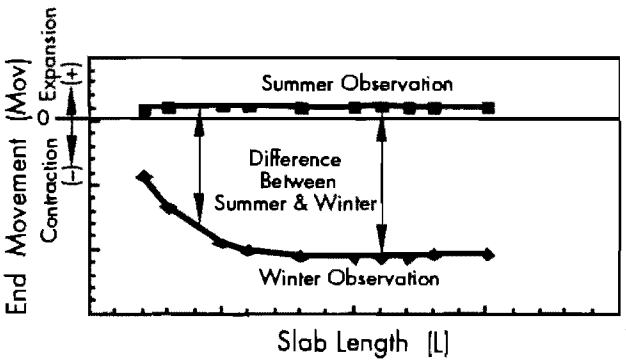

(a) The relationship of end movement and slab length observed in winter and summer

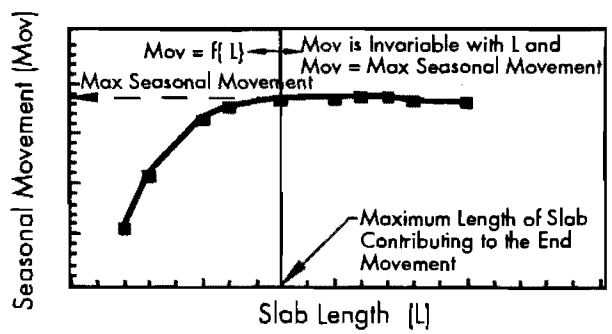

(b) The curve of difference between summer and winter

Figure 2.7 Relationship between end movement and slab length

Figures showing the relationship between end movement and slab length for each combination of

variables are found in Appendix A, with Figure 2.8 being a typical graph. In addition, Figure 2.8(b), which illustrates the case of an 8-inch-thick SRG aggregate slab placed in the summer over a subbase with a 4.6 psi friction force, will be the basis by which the effects of different variables are discussed in the following sections. Note that in the figure, the seasonal movement becomes invariant in relation to slab length at a value of 400 feet. Thus, the maximum length of the slab contributing to end movement is 200 feet.

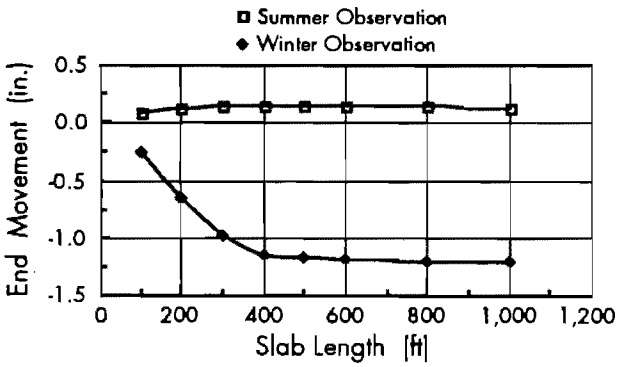

(a) End movement in relation to slab length

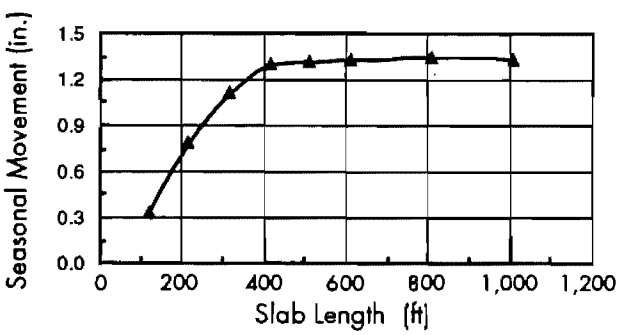

(b) Seasonal movement in relation to slab length

Figure 2.8 End and seasonal movements in relation to slab length for 8-inch-thick SRG aggregate slab placed in the summer over a subbase with a 4.6 psi friction force

In Tables 2.7 and 2.8, the maximum lengths of the slab contributing to end movements and the maximum seasonal movements are summarized for each set of variables. Note that in Tables 2.7 and 2.8 the maximum slab length of moving CRCP is one-half of the slab length at which the maximum seasonal movement becomes constant, which is shown by the figures in Appendix A. The maximum slab length of moving CRCP is the actual slab length that produces the maximum seasonal movement at one end.

2.5.1.2 Aggregate Type

Figure 2.9 was created by graphing an LS aggregate type on Figure 2.8(b). Figure 2.9 demonstrates, by holding other variables constant, a typical comparison of effects for two aggregate types, LS and SRG. For the same conditions, the end movement of the SRG aggregate is always greater than that of the LS aggregate. This is explained by the fact that the thermal coefficient of SRG is 1.33 times greater than the thermal coefficient of the LS aggregates (see Table 2.1).

Comparing Tables 2.7 and 2.8, we see that, between SRG and LS aggregates, there is only a minor difference in the maximum lengths of moving CRCP. Therefore, the slab lengths that contribute to end movement are almost the same, regardless of aggregate type.

Also, the maximum seasonal movement of the SRG aggregate is, on average, approximately 1.5 times the value of the LS aggregate. The value of the ratio of the maximum seasonal movement of SRG aggregate to the maximum seasonal movement of LS aggregate times 1.5 is greater than the value of the ratio of the thermal coefficient of SRG aggregate to the thermal coefficient of LS aggregate times 1.33. This is because more cases of full sliding and excessive movement occur with the SRG rather than with the LS.

Table 2.7 Summary of a study of CRCP end movement
Aggregate type: Siliceous river gravel

Subbase Type	Placement Season	Thickness of Slab (in.)	Maximum Slab Length of Moving CRCP (ft)	Seasonal Movement (in.)	Maximum Rate of Movement (in./°F)
Friction = 1.0 psi	Summer	8	1,000	5.81	0.0854
		12	1,250	8.70	0.1264
	Winter	8	750	3.83	0.0577
		12	1,000	5.78	0.0873
Friction = 4.6 psi	Summer	8	200	1.32	0.0184
		12	300	1.92	0.0282
	Winter	8	200	0.93	0.0130
		12	250	1.33	0.0197
Friction = 15 psi	Summer	8	100	0.46	0.0062
		12	150	0.66	0.0092
	Winter	8	100	0.36	0.0052
		12	100	0.49	0.0070

Table 2.8 Summary of a study of CRCP end movement
Aggregate type: Limestone

Subbase Type	Placement Season	Thickness of Slab (in.)	Maximum Slab Length of Moving CRCP (ft)	Seasonal Movement (in.)	Maximum Rate of Movement (in./°F)
Friction = 1.0 psi	Summer	8	800	3.75	0.0541
		12	1,100	5.53	0.0813
	Winter	8	600	2.45	0.0376
		12	800	3.61	0.0549
Friction = 4.6 psi	Summer	8	200	0.83	0.0122
		12	250	1.25	0.0181
	Winter	8	200	0.62	0.0092
		12	250	0.87	0.0134
Friction = 15 psi	Summer	8	100	0.32	0.0046
		12	100	0.40	0.0061
	Winter	8	100	0.27	0.0040
		12	100	0.35	0.0052

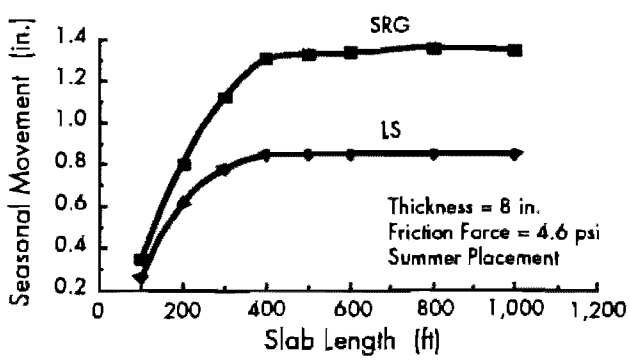

Figure 2.9 Typical seasonal movement in relation to slab length and a comparison between SRG and LS

2.5.1.3 Subbase Friction Force

Figure 2.10 was created by merging the other two friction force cases, 1.0 and 15.0 psi, with Figure 2.8(b). Figure 2.10 illustrates that a smaller friction force corresponds to greater end movement. This is consistent with expectations because, as the friction force decreases, the pavement movement meets less resistance so that the end movement increases. Thus, the friction force effect is significant for long CRC pavement slabs (see Tables 2.7 and 2.8), but not for short ones. This is explained by the fact that, if the slab length is short, the friction force will be in the elastic range and, thus, no sliding occurs.

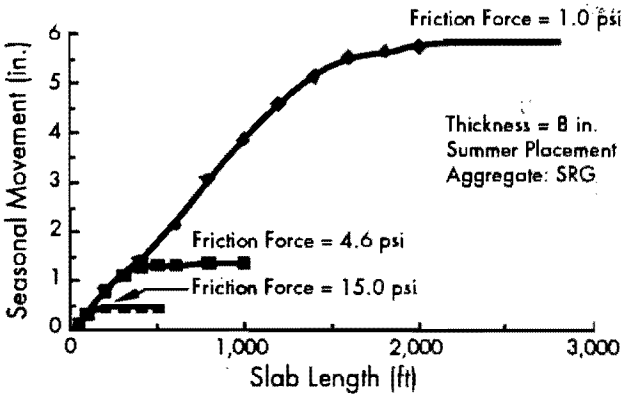

Figure 2.10 Typical seasonal movement in relation to slab length, and a comparison among three different friction forces

Figure 2.11 (from Figure 2.10) displays the effects of friction force on the maximum seasonal movement and on the maximum length of moving CRCP. When the differences among the three friction forces are compared for the same condition, a significant decrease in the end movement is found when the subbase friction is from 1.0 psi to 4.6 psi. When the subbase friction is from 4.6 psi to 15.0 psi, there is less of a decrease, as shown in Figures 2.11(a) and (b). Figure 2.11, then, indicates that the end movement is in the elastic range when the friction force is higher than 4.6 psi and that, possibly, the "break point" value is lower than 4.6 psi.

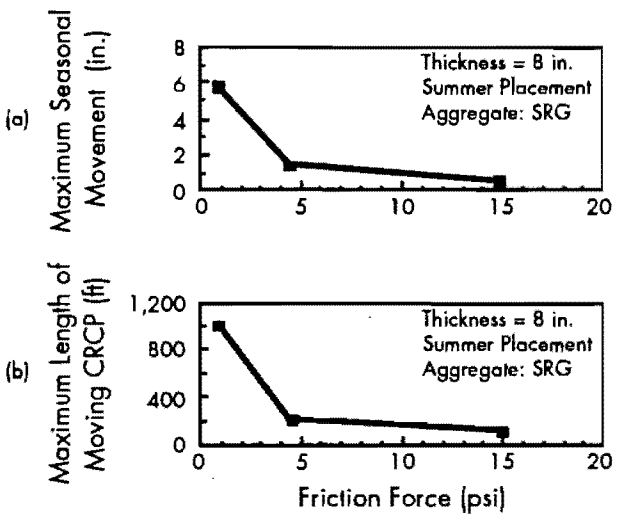

Figure 2.11 (a) Maximum seasonal movement and friction force, (b) maximum length of moving CRCP and friction force

2.5.1.4 Placement Season

Temperature change results in more expansion in the winter placement case and more contraction in the summer placement case. For total movement in a year, however, the winter placement can result in less end movement for the slab, as shown in Figure 2.12.

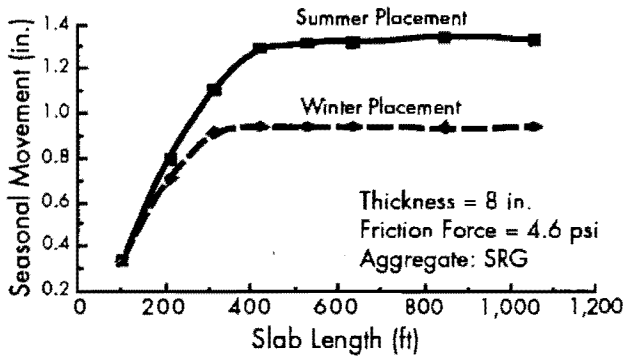

Figure 2.12 Typical seasonal movement in relation to slab length and a comparison between summer and winter placement

PSCP2 indicates there is more end movement in a slab placed in the summer than in the winter. This end movement for summer placement is caused by the inelastic range of the friction forces developing beneath long pavement slabs (Ref 11), a result of the longer overall temperature differentials. These temperature differentials could in fact be the cause of a long-term contraction. Thus, there is more contraction than expansion in the same temperature change. Since there is a higher setting temperature when the pavement is placed in the summer, the ratio of decreasing temperature to increasing temperature in the summer placement case is higher than that in the winter placement case. Although the yearly temperature change is the same, the summer placement case will have 1.33 times the end movement of the winter placement case.

2.5.1.5 Slab Thickness

Figure 2.13, created by merging a 12-inch slab with Figure 2.8(b), shows seasonal movements of 12-inch and 8-inch slabs. Results indicate that more total movement can result from the thicker slab than the thinner one, as depicted in Figure 2.13. The thicker slab produces a heavier weight and more volume, resulting in increased horizontal force and thus more movement. Moreover, the 12-inch CRCP has about 1.5 times the maximum seasonal movement of the 8-inch CRCP. The ratio of the maximum seasonal movement of the 12- and 8-inch CRCP is equal to the ratio of the two slab thicknesses, 12 and 8 inches. This contradicts

previous subbase friction studies, which have shown that frictional resistance is a fixed value and does not vary with slab thickness. (NOTE: Figure 2.13 is a computed graph; we would anticipate the plots based on Wimsatt's work that suggests the friction is constant regardless of pavement depth. See Ref 16.)

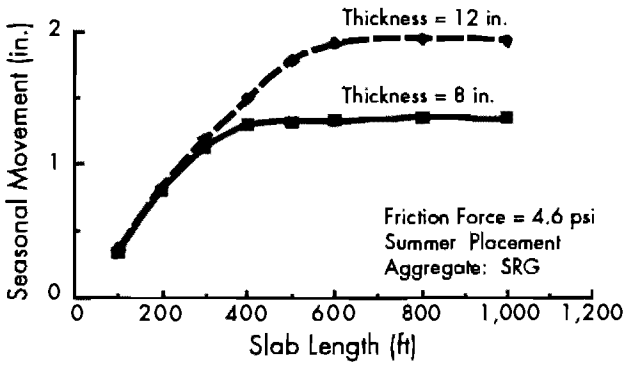

Figure 2.13 Typical seasonal movement in relation to slab length and a comparison between 8-inch and 12-inch slabs

2.5.1.6 Summary

Generally, the maximum end movement of a CRCP is directly related to temperature change and slab thickness, and is inversely related to subbase friction when one considers the total annual movement. Winter placement conditions and the limestone aggregate will generate less end movements, all other conditions being equal.

The conclusions derived from the set of conditions considered are as follows:

- The end movements with frictions of 4.6 psi or greater are more elastic, whereas those end movements with frictions of less than 4.6 psi have a much greater sliding tendency.
- The end movement of the SRG aggregate is 1.5 times the value of the LS aggregate.
- A winter placement reduces the end movement to approximately 0.75 times that of a summer placement.
- An end movement change that is affected by the slab thickness is approximately equal to the ratio of slab thickness.

2.5.2 End Movement in Relation to Slab Temperature

It has been found from previous study that a linear relationship exists between end movement and slab temperature (Refs 2 and 5). The slope of each line in Figure 2.14 represents the change in pavement length per degree change in temperature, that is, the rate of movement ($\Delta X/\Delta T$) for each combination of variables (Ref 2). To compare one combination of variables against another, the slope of the trend line can be used as an indicator. Therefore, the relationship of end movement and slab temperature was developed, and the slope was obtained. In addition, the slope may be used to compare the results from theoretical models and from field measurements.

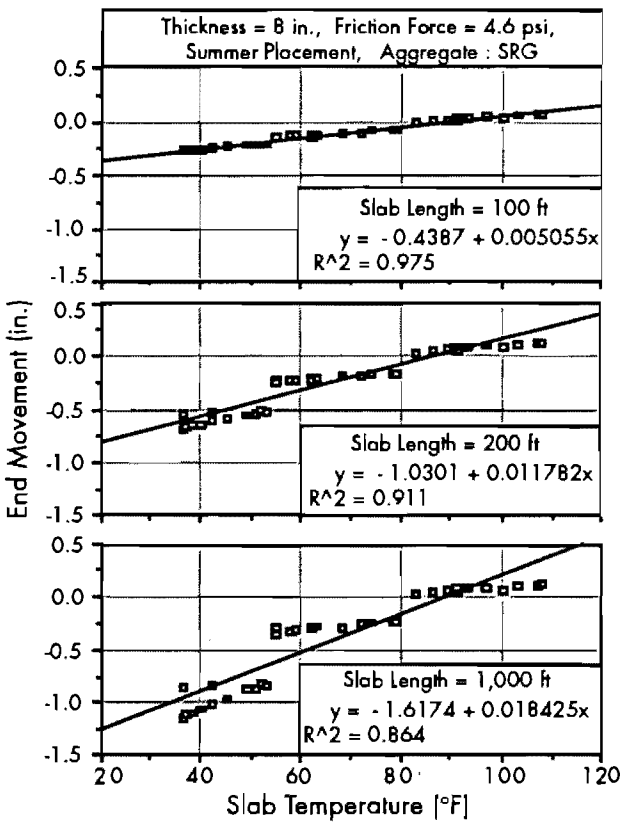

Figure 2.14 Typical end movement in relation to mid-depth temperature with different slab lengths

2.5.2.1 General Concept

In studying the relationship between end movement and slab temperature, we found that the slope increased, along with the slab length, under a certain combination of variables. Figure 2.14 indicates that the slope increases from 0.0050 to 0.0184, when the slab length increases from 100 to 1,000 feet. This is because the end movement increases with the slab length. Under the same temperature conditions, when the end movement increases, the rate of movement increases (i.e., the slope increases). Therefore, the rate of movement is related to the end movement. One could expect that the

relationship between the slope and the slab length follows the same pattern as that of the relationship between end movement and slab length. By comparing the daily and seasonal rates of movement in Table 2.9, however, it was observed that the variations in the daily rate of movement of the slab length were not as significant as those of the seasonal rate of movement. Thus, day-to-day movements are normally in the elastic range, and annual movements, as the seasons change, result in pavement sliding.

When the daily rates of movement listed in Table 2.9 are compared in different observation seasons, it is found that they are almost the same for 100-foot slabs, since a short slab generates less movement. The short slab movement remains in the elastic range regardless of temperature change. With longer slab length, the effect of the temperature change grows significantly and sliding occurs once the movement exceeds the elastic range. As the research has indicated (see Figure 2.6), a slab placed in the summer experiences greater temperature change, given the reference temperature of 87°F (see Table 2.5) observed in the winter. Thus, the rate of movement observed in the winter is greater than the rate of movement observed in the summer or the fall, especially for the 1,000-foot slab (see Table 2.9). For winter placement, the rates of movement observed in the summer and the winter are not as great as those observed in the winter for summer placement, owing to the 70°F reference temperature (see Table 2.5).

All of the figures describing the relationship between the slope and slab length are in Appendix B. In Figure 2.15, typical of these plots, the graph is similar to those representing the relationship between end movement and slab length. When a slab length exceeds a certain value, the slope is unaffected by slab length; that is, the interior of the slab is not moving if the slab is larger than the value in question. Figure 2.15 shows that the maximum slope is 0.018 for an 8-inch siliceous river gravel slab with a 4.6 psi subbase placed in the summer. The maximum slope is the maximum rate of movement for each combination of variables.

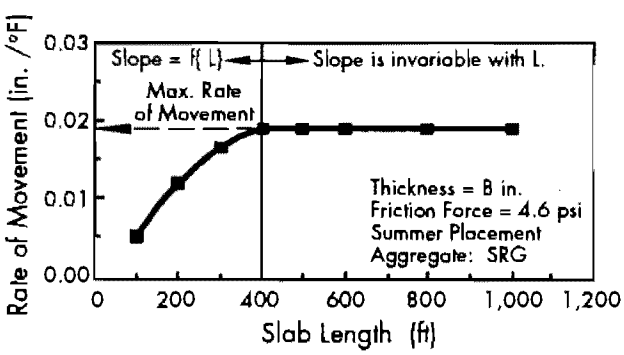

Figure 2.15 Typical curve of rate of movement and slab length

2.5.2.2 *Summary*

The maximum rate of movement for each combination of variables is listed in Tables 2.7 and 2.8. Since a slab length in excess of the maximum value would not influence the end movement, the rate of movement remains the same when the slab length exceeds the maximum value. This is another proof that end movement and the rate of movement share the same slab length relationship.

Table 2.9 Comparison of daily and seasonal rates of movement for 8-in. SRG aggregate slab placed over subbase with 4.6 psi friction force

Placement Season		Summer			Winter		
Slab Length (ft)		100	200	1,000	100	200	1,000
Daily Rate of Movement (in./°F)	Summer	0.0031	0.0035	0.0035	0.0031	0.0036	0.0045
	Fall	0.0030	0.0032	0.0039	0.0030	0.0032	0.0033
	Winter	0.0030	0.0067	0.0136	0.0030	0.0051	0.0060
Seasonal Rate of Movement (in./°F)		0.0051	0.0136	0.0184	0.0050	0.0107	0.0130

CHAPTER 3. ANALYSIS USING FIELD DATA

3.1 BACKGROUND

While the mechanistic computer program alone can make predictions of pavement terminal movement, such predictions are not totally error free. There remain those miscalculations—usually the result of faulty assumptions—made during the computer simulation process. The reliability of the results should therefore be verified with field data before using the computer results in design decisions. It is in fact through such an investigation of the field data that we gain a better understanding of the difference between the results obtained from the mechanistic model and those obtained from experiments. A correction that is predicated on such a difference can then be used to calibrate the computer model. In this way, we can account for the effects of terminal movements under various conditions in the design procedure.

A comparison of the field data with the results obtained from the mechanistic model requires measurements of free end pavement movements. In addition to longitudinal end movement, the transverse movement may also be measured.

Accordingly, the purpose of this chapter is to supplement Research Report 39-2 (Ref 2) field data on CRCP longitudinal end movement with more recent data. In this chapter, the field measurement is first presented; then, the data collected are described and analyzed.

3.2 FIELD INSTRUMENTATION AND DATA COLLECTION

In this section, the following will be discussed:

- the measurement section;
- the selection of the measurement locations;
- the measurement instrument; and
- the selection of the measurement time.

3.2.1 Description of Measurement Section

The continuously reinforced concrete pavement selected for measurement in Houston is on the main lanes of SH 225, just north of IH-610 (South Loop) at the point where the construction ends and the lanes "stub out" for future construction. The main lanes in one direction consist of a 10-foot median, four 12-foot main lanes, and a 12-foot shoulder. The four main lanes are numbered from median to shoulder. Figure 3.1 illustrates the plan view of the measurement section. There are longitudinal construction joints between the median and Lane 1, between Lane 2 and Lane 3, and between Lane 4 and the shoulder. The two sawed groove longitudinal joints in the section are between Lanes 1 and 2 and between Lanes 3 and 4.

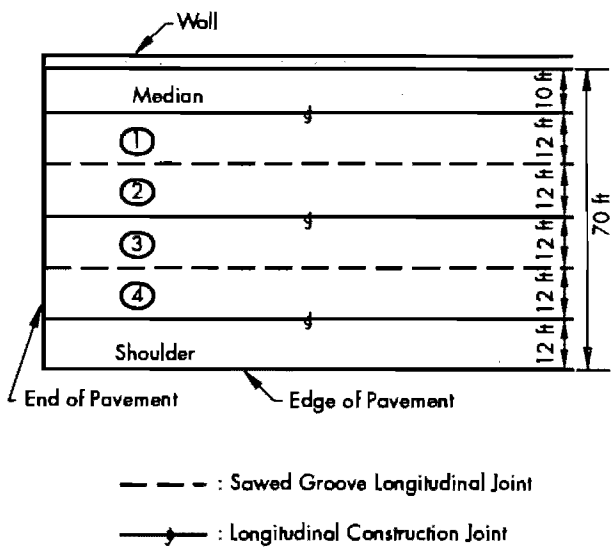

Figure 3.1 Plan view of the measurement section

According to the project plans, the pavement was placed in October 1974. It consists of 8 inches of continuously reinforced concrete pavement over 6 inches of asphaltic subbase; the measured slab is 1,000 feet. The aggregate material used in the paving concrete was siliceous river gravel. There are no terminal anchorages at the end of the slab, and there was no traffic on the measurement section. Hence, the slab—at one end and at each edge—can be considered a free end pavement.

3.2.2 Selection of Measurement Locations

The easiest way to observe pavement movement is to measure the relative distance of two fixed points periodically, with the change in the measured distances indicating the amount of movement. If the distance decreases, expansion occurs; if the distance increases, contraction occurs. To form a fixed point, a Demac point was epoxied on the pavement as depicted in Figure 3.2. It is obvious from Figure 3.3(a) that when a measurement is performed at a joint, two Demac points can be directly epoxied across that joint. When the measurement is performed at the pavement edge, however, only one Demac point can be epoxied. In such cases, a fixed reference point is needed. As shown in Figure 3.3(b), this reference point was made by drilling a 4-inch-diameter core and inserting a 1-inch-diameter, 3-foot-long rebar into a layer of soil.

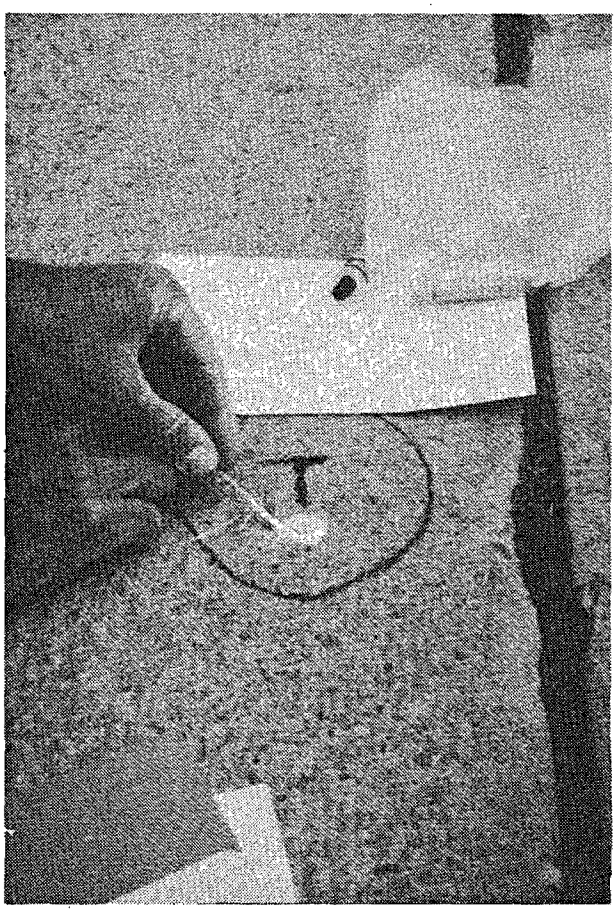

Figure 3.2 Fixed point set-up

Figure 3.3(a) illustrates a plan view of the measurement locations. A measurement location is formed by a set of two fixed points. Locations A through E, selected for the measurement of transverse movement, were placed about 76.5 feet from the end of the pavement. Locations A, B, and D were chosen for measuring movement change in a construction joint where the movement is restricted by tie bars, as shown in Figure 3.3(d). To compare the movement at two different joint types, we measured the movement change at the Location C sawed groove joint shown in Figure 3.3(c). The Location C movement is restricted not only by the steel rebar, but also by the degree of cracking. The transverse end movement was measured at Location E at the pavement edge. Since Lane 1 and Lane 3 were 1,000-foot rectangular slabs, we selected them for end movement measurement. The measurement locations at the end of Lanes 1 and 3 were designated F and G, respectively. Data from E, F, and G can be compared with the computed values in Chapter 2 for matching conditions.

3.2.3 Description of the Instrument

We used a multi-position strain gauge and a standard bar to measure pavement movement. The multi-position strain gauge is operated by inserting the points of the gauge into the holes in the center of the Demac points, with the reading then recorded. Figure 3.4 shows the movement measurement derived from the gauge.

The multi-position gauge (whose accuracy is 0.001 inch) was often adversely affected by environmental factors. To correct for any errors resulting from these factors, we used the standard bar. Figure 3.5 shows the dial gauge and the standard bar at the location of two Demac points across a joint, while Figure 3.6 shows the measurement between a Demac point and a fixed reference point.

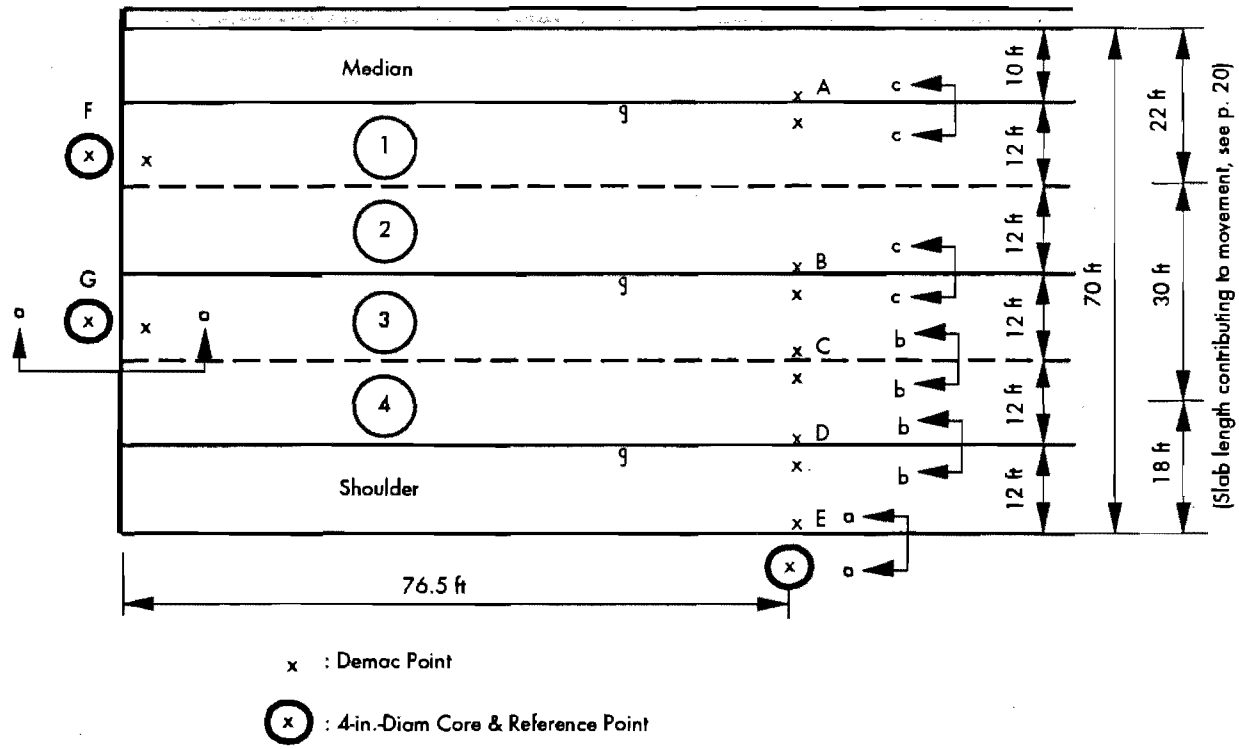

(a) Plan View

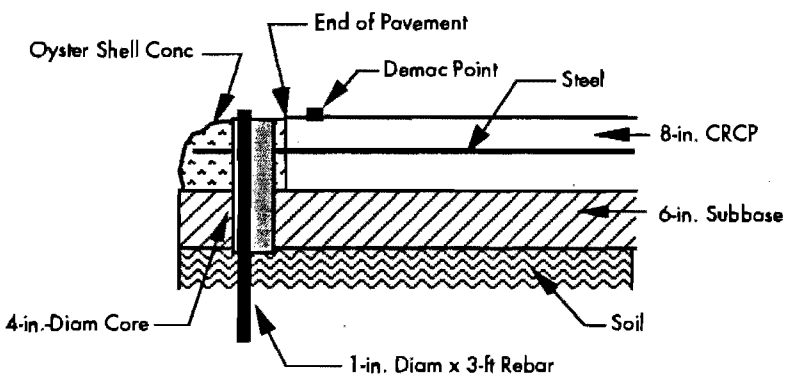

(b) Section a-a

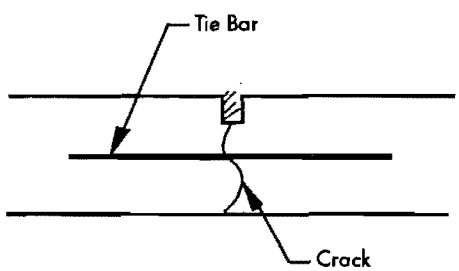

(c) Section b-b

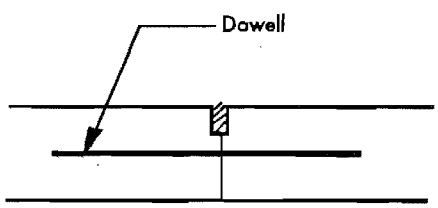

(d) Section c-c

Figure 3.3 (a) Plan view of measurement location, (b) cross section of the reference point, (c) cross section of sawed joint, (d) cross section of construction joint

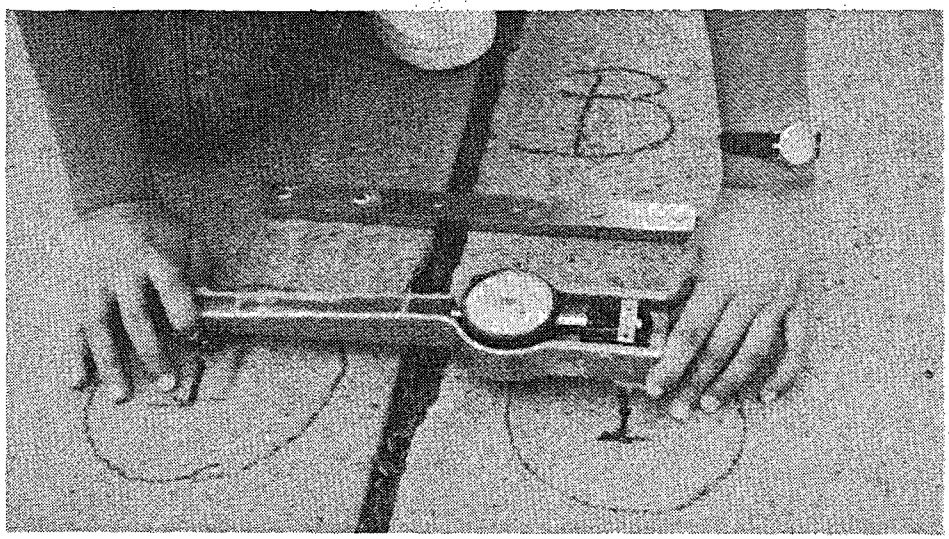

Figure 3.4 Movement measurement using dial gauge

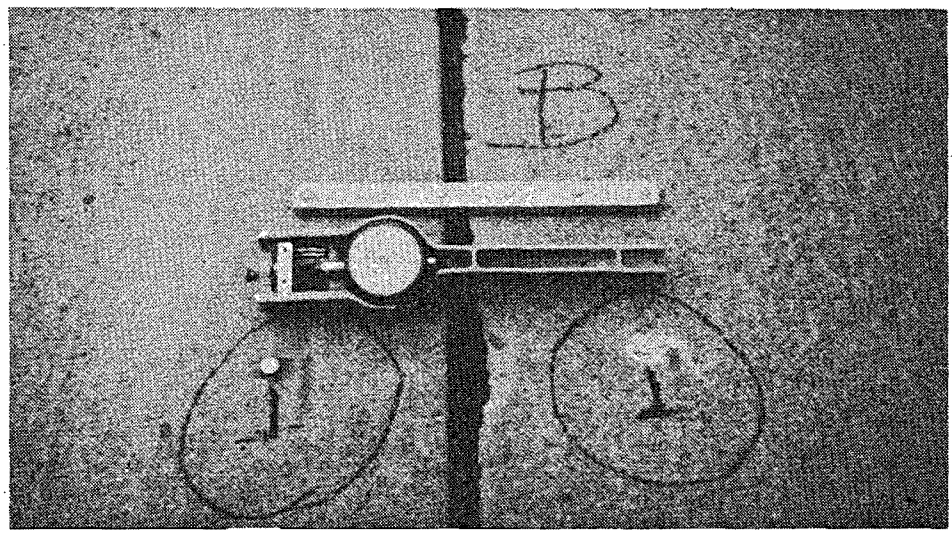

Figure 3.5 The placement of Demac points across a joint and the dial gauge used in the measurement

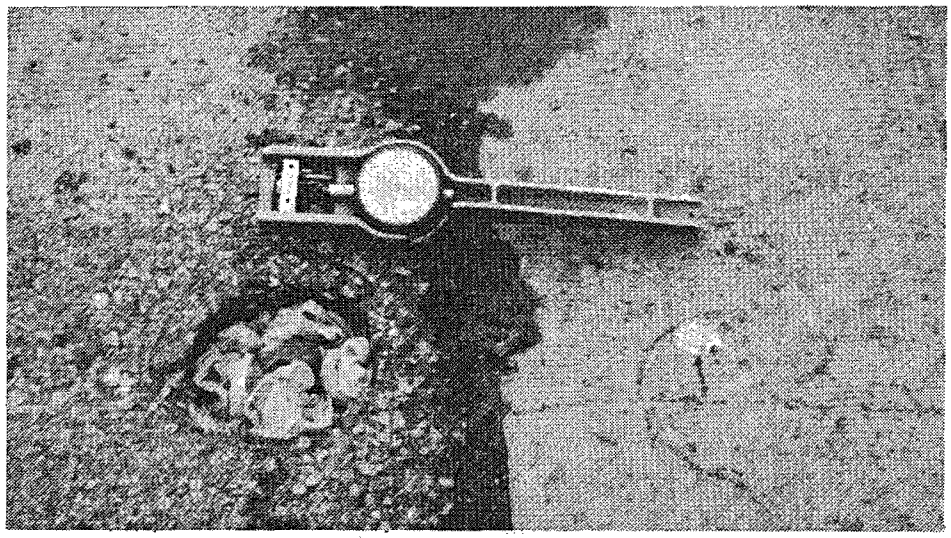

Figure 3.6 The measurement between a Demac point and a fixed reference point

Thermocouples were positioned 1 inch from the surface, at mid-depth, and 1 inch from the bottom of a block of 10-inch-thick concrete. The concrete block was embedded into the soil to simulate the concrete slab at the measurement section (Refs 9 and 10). A thermometer was used to measure the concrete temperatures at three depths within the concrete block, as shown in Figure 3.7. The air temperatures were also obtained from the thermometer. Temperature and multi-position strain gauge readings were recorded simultaneously.

3.2.4 Selection of Measurement Time

In a daily temperature cycle, the lowest temperature generally occurs at sunrise, and the highest temperature occurs approximately 2 hours after noon. Figure 3.8 demonstrates the daily temperature cycle for the project. Data were collected at 1-hour intervals from 6:00 a.m. to 6:00 p.m., so that the highest and lowest temperatures—corresponding to maximum expansion and contraction—could be included.

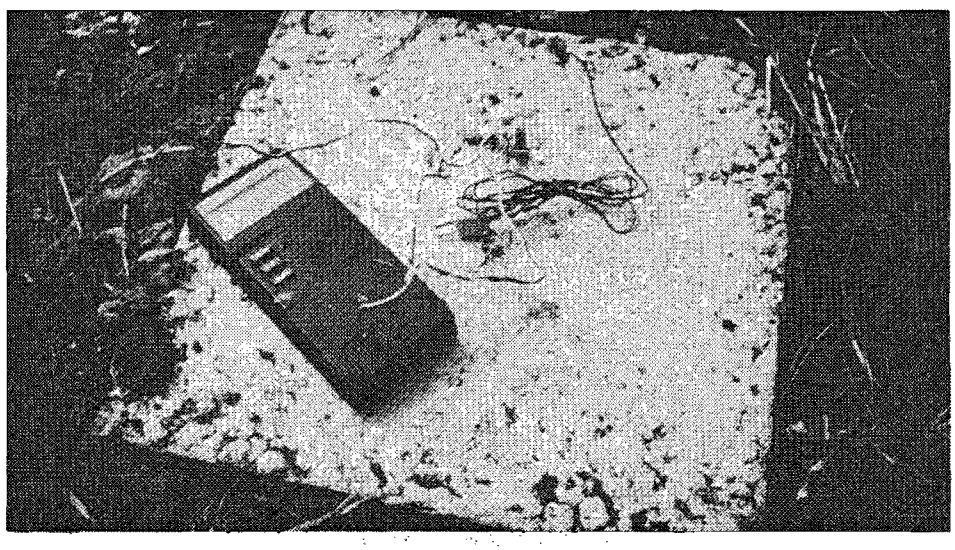

Figure 3.7 Instrument used for temperature measurement

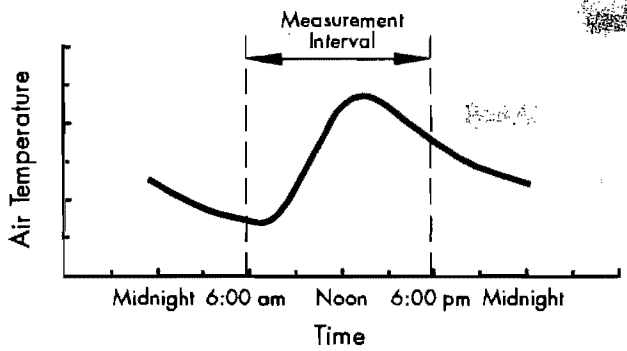

Figure 3.8 Air temperature in relation to time on daily basis

3.3 DATA PRESENTATION

Appendix C presents gauge plug measurements, air temperatures, and concrete temperatures. Note that, while air and concrete temperatures were measured, only concrete temperatures were used for analysis. Since the material in the dial gauge was temperature sensitive, the dial gauge reading varied with the temperature when two equal distances were measured. To maintain accuracy, the dial gauge readings of a pair of gauge plugs were compared under the same circumstances with the dial gauge reading of a 10-inch-long standard bar unaffected by temperature. All data for the gauge plug readings shown in Appendix C were corrected.

3.4 DATA ANALYSIS

This section discusses the statistics used for a linear regression analysis of the field data collected on SH 225 in Houston. The purpose of the linear regression analysis is to identify the relationship between the gauge plug reading and temperature, i.e., the relationship between the horizontal movement of pavement and temperature.

3.4.1 Statistical Analysis

To establish the relationship between the gauge plug readings and slab temperature, we plotted the gauge plug readings in relation to the slab temperatures. (The plots from all the measurement locations are contained in Appendix D.) Figure 3.9 shows a typical plot of the gauge plug readings in relation to the slab temperatures. It can be seen from the plot that a linear relationship exists between the gauge plug reading and the slab temperature. In this way, we obtained the linear regression equations presented in Table 3.1.

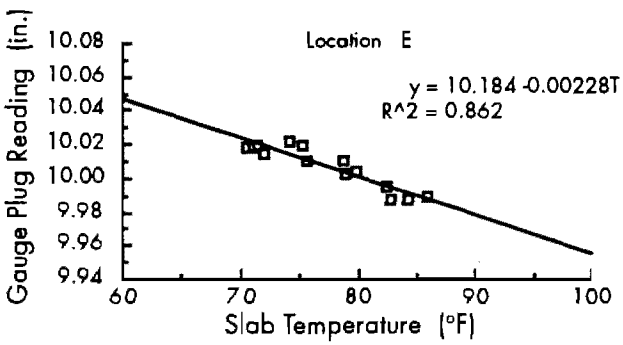

Figure 3.9 Gauge plug reading and slab temperature

In Table 3.1, the linear equations are expressed as follows:

$$Y = a - bT$$

where: Y = gauge plug reading, inches,
T = slab temperature, °F,
a = Y-intercept, and
b = the slope of the line, $\frac{\Delta Y}{\Delta T}$.

Note that the slope of regression line b can also explain the change in the length of the pavement (i.e., the rate of movement) per degree change in slab temperature. Thus, the b term forms an indicator that compares pavement movement among all the measurement locations.

Table 3.1 Linear regression equations and R^2 values

Measurement Location	Type of Joint	Regression Equation	R^2 Value
A	Construction joint	Y = 10.151 - 0.00193T	0.923
B	Construction joint	Y = 10.246 - 0.00279T	0.979
C	Sawed joint	Y = 10.036 - 0.00038T	0.667
D	Construction joint	Y = 10.052 - 0.00045T	0.670
E	Free edge	Y = 10.184 - 0.00228T	0.862
F	Free end	Y = 10.693 - 0.00970T	0.869
G	Free end	Y = 10.797 - 0.01121T	0.873

Table 3.1 also shows the R^2 values obtained from regression analyses. The value of R^2 indicates how well the regression line fits the data, with a value of 1.0 being a perfect fit. Because most of the values are greater than 0.85, the regression line fits the data very well. Even when the R^2 values drop to around 0.65 (at Location C and Location D), the regression line still gives a reasonable fit to the data.

3.4.2 Transverse Movement

Figure 3.10 illustrates the transverse movements at different locations. By comparing the slopes of the transverse movements, it can be seen that the rates of movement at Location C and at Location D are much less than those at other locations. Figure 3.11 shows that Locations A, B, and E are at the construction joints and the pavement edge. Note in Figure 3.3, which is based on the project's plans, that Location A and Location B have dowels and that Location E is at a free edge, whereas Location C and Location D have tie bars that restrict their movement. Thus, there is more movement at Locations A, B, and E. Although Location D is also a construction joint, it can be considered as a sawed groove joint such as Location C since there is a tie bar which is well-bonded to the concrete. Hence, the behaviors characterizing Location C and Location D are similar.

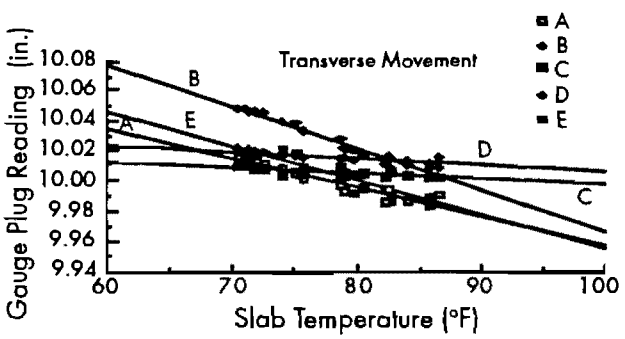

Figure 3.10 Gauge plug reading in relation to slab temperature at Locations A through E

The daily movements for each location are presented in Figure 3.11. Because the measurements are taken during the daily cycle, the difference between the extreme contraction and the extreme expansion can represent daily movement. The values indicate how far the pavement joints move during one day.

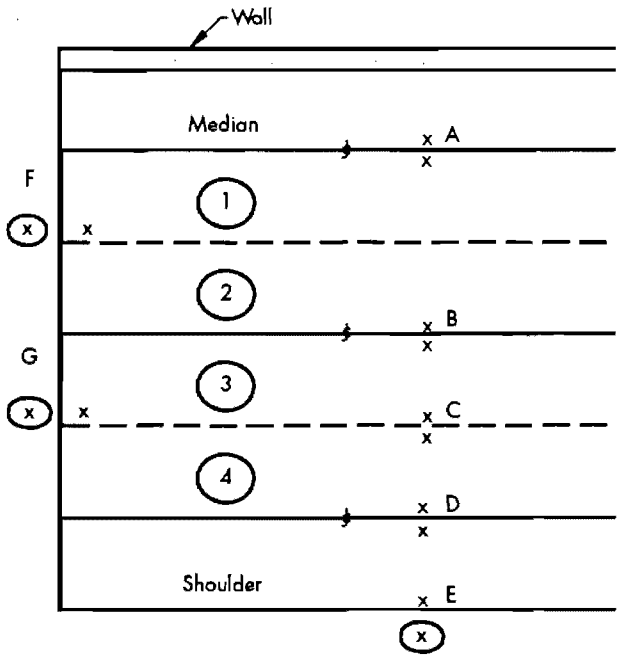

Transverse Movement		
Location	Daily Movement (in.)	Rate of Movement (in. /°F)
A	0.0312	-0.00193
B	0.0405	-0.00279
C	0.0089	-0.00038
D	0.0101	-0.00045
E	0.0347	-0.00228

Figure 3.11 Summary of daily movement and rate of movement for transverse direction

Figure 3.12 shows the relationship between rate of movement and slab length contributing to movement. The selected points, Locations A, B, and E, are either at a free end or at a joint whose behavior is like a free end. Hence, three free end movements are compared. The result indicates that the rate of movement increases as more slab length contributes to movement. The result is consistent with a longitudinal-direction relationship. It should be noted that the slab length contributing to end movement means that half of the slab length is affecting the movement. Although the movement is in a transverse direction, it can be considered, since there are three slabs in the same direction, i.e., a slab from Location E to Location B, a slab from Location B to Location A, and a slab from Location A to the wall (see Figure 3.3), with Location A and

Location B being joints. Therefore, at Location E only half of the first slab contributes to the movement, since it is at the edge of the slab. (And since Location E is at a free edge, its movement is greater that than at Location A, as shown in Figure 3.12.) At Location A and Location B, there are two slabs affecting movement, so that the slab length contributing to end movement at these two locations is half the total length of the two slabs.

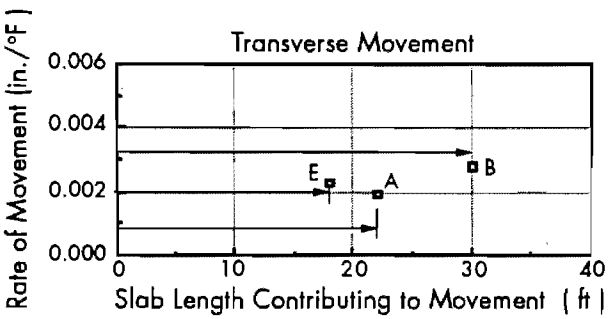

Figure 3.12 Rate of movement and slab length contributing to movement in transverse direction

3.4.3 End Movement

Figure 3.13 shows the longitudinal end movement at Location F and at Location G. Because the difference between the slopes of the two measurement locations is so small, the end movements can be considered essentially equal. Figure 3.14, a listing of the daily movement and rate of movement, shows that the average daily movement of a 1,000-foot CRCP is as much as 0.15 inch. One could expect that there is much more movement over a year. The average rate of movement on a daily basis is about 0.01 in./°F.

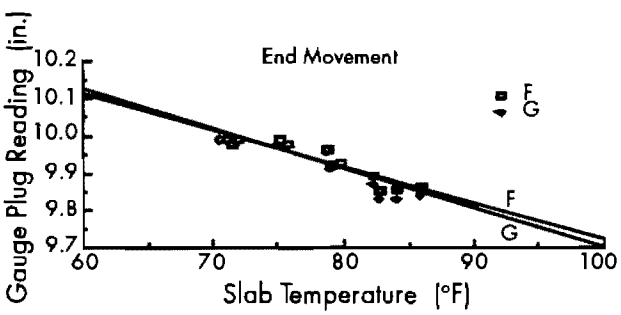

Figure 3.13 Gauge plug reading in relation to slab temperature at Location F and Location G

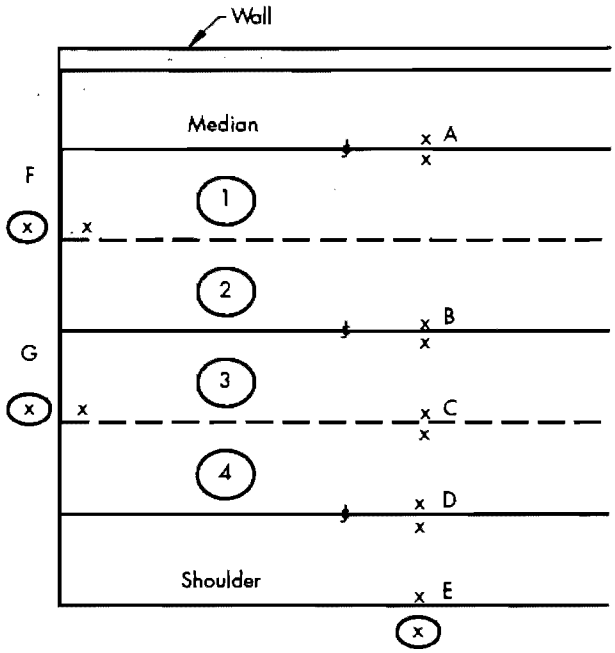

End Movement		
Location	Daily Movement (in.)	Rate of Movement (in./°F)
F	0.1401	-0.00970
G	0.1608	-0.01121
Average	0.1505	-0.01046

Figure 3.14 Summary of daily movement and rate of movement for longitudinal direction

3.4.4 Summary

The previous analysis has shown that the horizontal movement is not significant in the sawed groove joint, owing to the fact that the steel across the joint is well bonded. This observation can be verified by the lack of significant movement at Location D, which is a construction joint. Thus, well-bonded steel resists movement.

End movement measurements have shown that free end movement is significant. The next chapter compares these end movement measurements with the results obtained from the mechanistic model.

CHAPTER 4. COMPARISON OF MECHANISTIC RESULTS WITH FIELD DATA

4.1 BACKGROUND

In Chapter 2, the end movements of CRCP were predicted using the PSCP2 program. In verifying the reliability of those computer predictions, this chapter compares predicted movements with actual movements. In addition, it presents the calibrated result of subbase friction.

As described in Chapter 3, we obtained actual CRCP movements through a field measurement exercise that involved only one CRCP subbase type. Because comparing the computer predictions with a large database requires measurements obtained from different subbase types, we made use of the findings of Research Project 39, "Evaluation of Terminal Anchorage Installations on Rigid Pavements," conducted by the Highway Design Division at the Texas Department of Transportation (Refs 1 through 4). In that project, long-term end movement measurements of CRCP constructed on different subbase types were taken across Texas. The results from Research Project 39 will thus be compared with predicted end movements.

4.2 DESCRIPTION OF COMPARED DATA

The end movement data obtained for different temperature changes were from different field data sources; consequently, the end movements were not comparable. In order to gain some benefit from these data, we used a single temperature change as a standard: the rate of movement—that is, the end movement per Fahrenheit degree (in./°F)—was selected as the standard by which to compare these data. Thus, all the data displayed in this section are rates of movement. This section will present and discuss the data used for comparison.

4.2.1 Field Data

The two sources of field data are SH 225 in Houston and Research Project 39. Because most of the CRCP's tested in Texas 20 to 30 years ago are 8 inches thick, we used only that thickness of CRCP in the comparison. Additionally, siliceous river gravel (SRG) is the only aggregate present in these measured pavements. The primary difference between these data sources is subbase type (i.e., friction force between the subbase and the CRCP). The following sections present the field data.

4.2.1.1 SH 225 in Houston

All of the measurements conducted at SH 225 in Houston were described in Chapter 3. Locations E, F, and G (at the free edge or a free end) were selected for comparison with the predictions from the PSCP2 mechanistic model. Table 4.1 shows the three locations' relative pavement information and their rates of movement.

4.2.1.2 Research Project 39

Research Report 39-4 (Ref 4) contains the rates of CRCP end movement for three subbase types. Friction forces of 15 psi and 4.6 psi were programmed into the computer for cement-stabilized and asphalt-stabilized bases, respectively. Since the effect of terminal lugs cannot be evaluated by the PSCP2 program, only the data for CRCP's with zero terminal lugs were selected.

Project 39 data are shown in Table 4.1. It should be noted that because the data did not indicate the placement seasons for the CRCP in the project, the average rates of movement for

Table 4.1 Field data and rates of movement for continuously reinforced concrete pavement

Data Source	Subbase Type	Placement Season	Slab Length (ft)	Rate of Movement (in./°F)
SH 225 Location E	Asphaltic	Fall	40	0.0023
SH 225 Location F	Asphaltic	Fall	1,000	0.0097
SH 225 Location G	Asphaltic	Fall	1,000	0.0112
Project 39	Asphalt Stabilized	Winter	400	0.0056
Project 39	Cement Stabilized	Fall*	>500	0.0068
Project 556	Polyethylene	Fall*	240	0.011
Project 556	Polyethylene	Fall*	440	0.023

*The average rate of movement can be considered as that movement measured in the fall or spring.

each subbase type were chosen. If the quantity of the data is large enough, the average rate of movement can be generally considered as that rate of movement obtained from CRCP's placed in the fall or the spring (because fall and spring movement measurements fall midway between those extreme measurements recorded for summer and winter). Therefore, the fall placement was chosen for the cement-stabilized subbase case, which is shown in Table 4.1. For the asphalt-stabilized subbase case shown in the table, however, only three rates of movement from the 400-foot slabs are available (all of them very low). For the purpose of comparison, the average value for the asphalt-stabilized subbase case is the same as the average value for the CRCP placed in the winter.

Since there are no field data of the polyethylene sheeting subbase from Project 39, the field data of the polyethylene case from Project 556 were selected and listed in Table 4.1.

4.2.2 *Predicted Data*

In order to match and to compare the conditions of the selected field data, we chose predicted data having the same conditions. These data are shown in Table 4.2. For the three fall placement cases, the average rates of movement for winter and summer placements were used. All of the rates of movement shown in the table are from the 8-inch slabs.

Table 4.2 Predicted rates of movement for different types of continuously reinforced concrete pavement

CRCP Type			
Subbase Friction Force (psi)	Placement Season	Slab Length (ft)	Rate of Movement (in./°F)
4.6	Fall*	40	0.0021
4.6	Fall*	1,000	0.0157
4.6	Winter	400	0.0130
15.0	Fall*	>500	0.0057
1.0	Fall*	400	0.0120
1.0	Fall*	400	0.0200

*The rate of movement for fall placement is the average rate of movement for winter and summer placement derived from the PSCP2 program.

4.3 RESULTS OF COMPARISON

The predicted rates of movement can be plotted in relation to field replicates that have equal parameters (e.g., subbase type, slab thickness, and placement season). Ideally, if there were no difference between the predicted rate of movement and the field data, the points would describe a 45-degree line. Figure 4.1 shows a plot of this type.

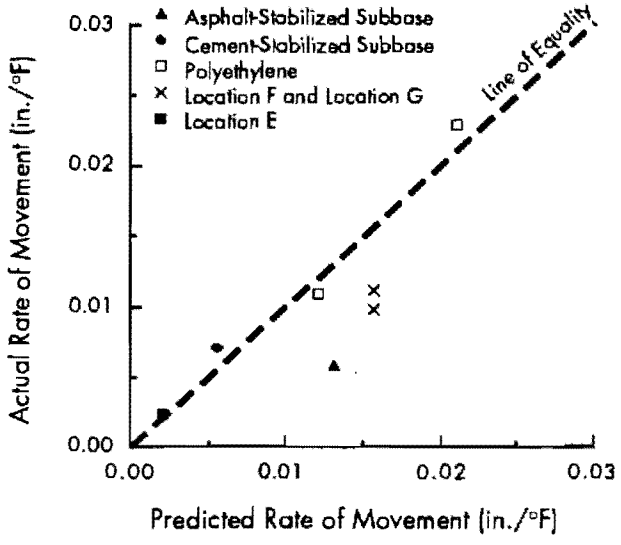

Figure 4.1 Predicted rates in relation to actual rates of movement

As shown in Figure 4.1, the computer program predicts the cement-stabilized subbase, polyethylene, and Location E cases very well, since the two points are on or near the 45-degree line. The other two cases, especially the case of the asphalt-stabilized subbase, are below the line of equality. This means that the predicted value is higher than the field value in the two cases. In other words, the field friction forces in the two cases are greater than those input into the predicted model. In order to correct the friction error, we performed the friction calibration described in the next section.

4.4 CALIBRATION

All the values of subbase friction used in the computer input were based on Research Report 459-2F (Ref 16). Every value represents a specific subbase type. Although the experimental values of subbase friction have been measured for years, it is still difficult to determine the values of subbase friction in the field because of the difference between subbase conditions in the laboratory and subbase conditions in the field. This difference between laboratory and field conditions is the cause of the discrepancy between predicted and measured values of end movement when a test value of subbase friction is input into the theoretical model. In order to correct this discrepancy, a calibration of subbase friction is performed.

The best way to pinpoint the friction force in the field is to create a relationship between rate of movement and friction force, followed by curve interpolation. Figures 4.2 and 4.3 illustrate the relationships between rate of movement and friction force for the asphaltic subbase of SH 225 and the asphalt-stabilized subbase used in Project 39. After interpolation, we obtained the calibrated values of field friction forces.

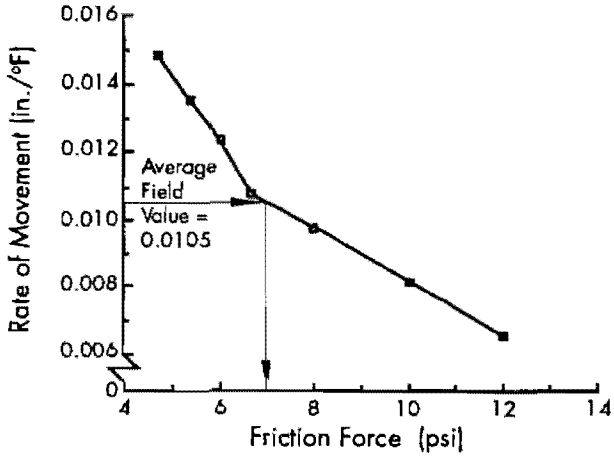

Figure 4.2 Relationship between rate of movement and friction force for CRCP on asphaltic subbase for the SH 225 Project

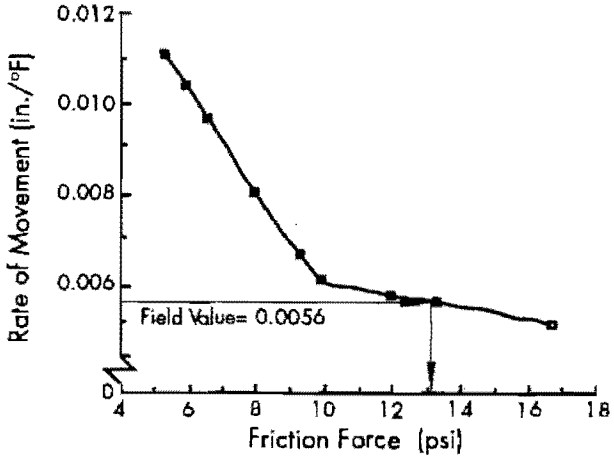

Figure 4.3 Relationship between rate of movement and friction force for CRCP on asphalt-stabilized subbase for Project 39

These calibrated values are listed in Table 4.3. Note that the value, 0.0105, used in Figure 4.2 for interpolation is the average rate of movement of Location F and Location G.

Table 4.3 Calibrated friction forces

Pavement Type		Friction Force (psi)
Length (ft)	Subbase Type	
1,000	Asphaltic	7.0
400	Asphalt stabilized	13.3

Although the two subbase materials are asphalt, the friction forces listed in Table 4.3 are quite different (7.0 psi and 13.3 psi). This difference may be explained by the 20-year interval separating their construction—an interval long enough to allow the adverse effects of aging and aggregate polishing to develop. Since the CRCP was built about 30 years ago, it is difficult to identify, specifically, the differences between the two asphalt subbases. Yet, it is obvious that they are different.

4.5 SUMMARY

Through comparison and calibration, we have verified the results obtained from the PSCP2 computer program. As long as the actual friction force in the field is known, the PSCP2 computer program can predict accurately the end movement. Since a computer-predicted end movement is greater than an actual end movement, it is probably true that the friction forces derived from experiments in Research Report 459-2F (Ref 16) are less than the actual friction forces in the field. While actual end movement should be further investigated, the friction force values reported here are reliable. Accordingly, a longitudinal joint device can be designed to accommodate projected end movements.

CHAPTER 5. IMPLEMENTATION

5.1 INTRODUCTION

Chapter 4 demonstrated that the predictions of the PSCP2 computer program compared favorably with the field data. Thus, the PSCP2 mechanistic model can be used to predict free end movement of CRCP's and, because of this capability, to design a superior road surface. The pavement designer may now compute the terminal movement of a slab to design joint dimensions and sealant types that fit specific site conditions. If the movements are too great, the designer may consider restricting the movement using terminal anchorages or other devices. For the convenience of pavement designers who have the responsibility of estimating terminal movement in CRCP, a design equation and design charts based on the analyzed results of the PSCP2 program may be developed.

The factors affecting the movement of pavement terminals, based on the data analysis in Chapter 2, are pavement length, temperature change, pavement thickness, aggregate type, season of placement, and subbase friction. The charts in Appendix A and Appendix B provide terminal movement estimations of different pavement lengths and with different combinations of factors. However, the CRCP is long enough to generate a constant end movement. In this chapter, the design chart and design equation will focus on CRCP—irrespective of pavement length.

This chapter, then, describes the implementation of the PSCP2 mechanistic model. The design equation and design charts, developed to estimate the terminal movement in CRCP, will contain the parameters already mentioned (with the exception of pavement length).

5.2 DEVELOPMENT OF DESIGN EQUATION

In Chapter 2, we demonstrated that a linear relationship exists between end movement and slab temperature, such that the rate of movement, $\Delta X/\Delta T$ (in./°F), is a constant; that is, the temperature change is directly proportional to the total end movement. The proportionality can be stated as follows:

$$\Delta X \propto \Delta T \qquad (5.1)$$

where: ΔX = total end movement, inches, and
ΔT = temperature change, °F.

By comparing the total end movement of 8- and 12-inch CRCP's in Chapter 2, we further demonstrated that the thickness of CRCP is also directly proportional to the total end movement. Accordingly, the proportionality is stated as follows:

$$\Delta X \propto D$$

where: D = thickness of CRCP, inches.

For the convenience of calculation, the proportionality can be normalized to a standard thickness, since a linear correlation of movement and thickness has been demonstrated in Chapter 2. This normalization may be accomplished by dividing with a standard thickness; for example, if 8 inches is used, the equation is as follows:

$$\Delta X \propto \frac{D}{8} \qquad (5.2)$$

In Chapter 2, it was shown that as the thermal coefficient increases from 6×10^{-6} in./°F (LS aggregate) to 8×10^{-6} in./°F (SRG aggregate), the total end movement increases to 1.5 times. The relationship between total end movement and thermal coefficient can be expressed by the following:

$$\Delta X \propto (\alpha_c)^{1.5}$$

where: α_c = thermal coefficient, in./°F.

For the convenience of calculation, the proportionality can be normalized by dividing with a constant, 6×10^{-6}, for example,

$$\Delta X \propto \left(\frac{\alpha_c}{6\times10^{-6}}\right)^{1.5} \qquad (5.3)$$

If we consider three parameters—temperature change, thickness of CRCP, and thermal coefficient—at the same time, the following proportionality can be obtained:

$$\Delta X \propto \frac{D}{8}\left(\frac{\alpha_c}{6\times10^{-6}}\right)^{1.5}\Delta T$$

$$\Delta X \propto A\frac{D}{8}\left(\frac{\alpha_c}{6\times10^{-6}}\right)^{1.5}\Delta T$$

where: A = constant of proportionality.

However, the constant A consists of two parameters: one for season of placement and one for subbase type. Therefore, we can convert A as follows:

$$A = a \bullet k$$

where: a = parameter of placement season, and
k = parameter of subbase type.

Thus, based on the results obtained in Chapter 2, we can show that the design equation is as follows:

$$\Delta X = a\frac{D}{8}\Delta T\left(\frac{\alpha_c}{6\times10^{-6}}\right)^{1.5}k \qquad (5.4)$$

Placement season parameters for summer and winter are listed in Table 5.1. Since the CRCP placed in the summer produces 1.33 times the total end movement of the CRCP placed in the winter, the value of the placement season parameter, a, for winter placement is 1.0, and the value for summer is 1.33. In addition, the total end movement also varies with subbase type. The values of subbase type parameters are listed in Table 5.2.

Table 5.1 Parameters of placement season

Season of Placement	Summer	Winter
a	1.33	1.0

Table 5.2 Parameters of subbase type

Type of Subbase	Polyethylene	ACB	CTB
k	0.0370	0.0086	0.0031

To verify the end movement computed by the design equation (5.4), we plotted in Figure 5.1 the relationship between the end movements of CRCP derived from Equation 5.4 and the end movements obtained from the PSCP2 program. This figure indicates that the design equation (5.4) can estimate the end movement of CRCP as accurately as the PSCP2 computer program. Thus, the design equation (5.4) can be used to estimate the end movement of CRCP.

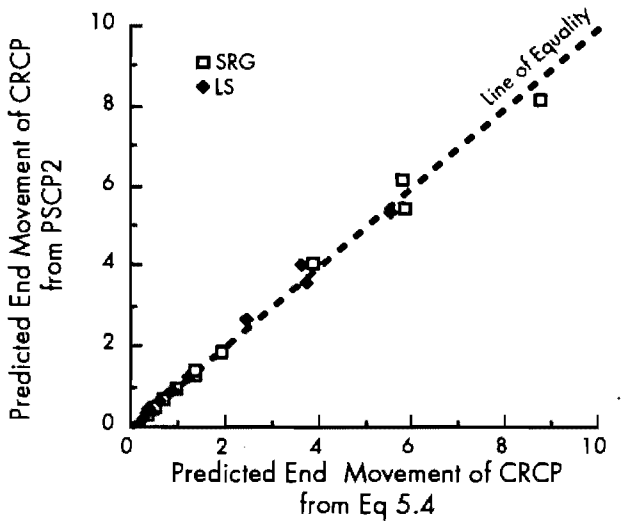

Figure 5.1 Predicted end movements of CRCP from PSCP2 in relation to predicted end movements of CRCP from Eq 5.4

Note that since this study focuses on CRCP constructed in Texas, the values input into each item in the design equation (5.4) must be in the range of what was discussed in Chapter 2.

5.3 IMPLEMENTATION OF THE MECHANISTIC PSCP2 MODEL

It is the designer's job to accommodate the terminal movement of a CRCP for a specific project. The first phase in the process is a more global evaluation of the problem. Next, a specific project evaluation should be made for quantifying the exact magnitude of the problem.

5.3.1 Overview Evaluation Procedure

Since the complexity of the design equation renders it impractical, design charts (Figures 5.2(a) and (b)) were drawn up to estimate the total end movement. Figure 5.2(a) is for SRG aggregate type and Figure 5.2(b) for LS aggregate type. There are two scales of total end movement for each type of aggregate: the one on the left is for 8-inch CRCP and the one on the right is for 12-inch CRCP. In each chart, there are three subbase types: polyethylene, ACB, and CTB. For each subbase type, there are two placement seasons: the solid line is for summer placement and the dashed line is for winter placement.

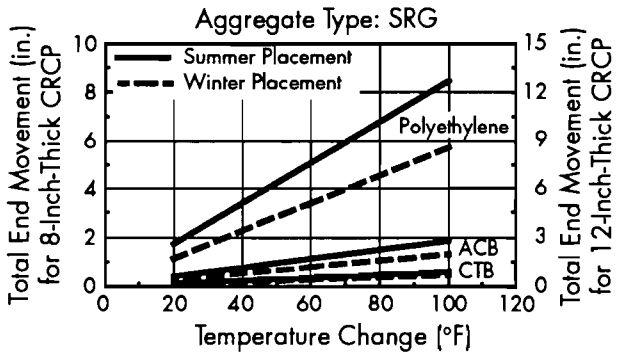

(a) Total end movement design chart for SRG aggregate

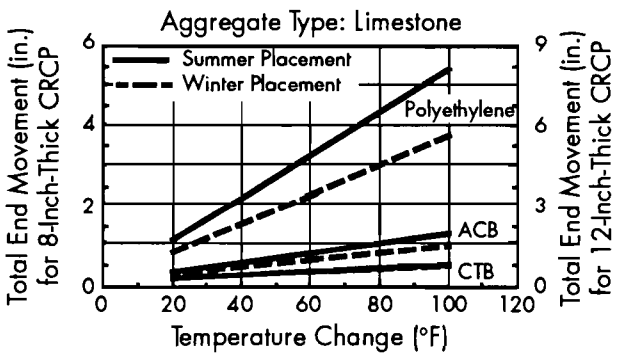

(b) Total end movement design chart for limestone aggregate

Figure 5.2 Total end movement design charts for CRCP

Note that the terminal movements are dependent on the magnitude of the variables at a specific location, making the design unique. Thus, the designer should recognize that a specific sealant and particular dimensions performing satisfactorily at one location may perform unsatisfactorily at another location.

In using the design charts to obtain the total end movement for the designed CRCP, pavement designers should input the seasonal temperature change, the aggregate type, slab thickness, and subbase type for the CRCP. For most installations, the total annual movement will be less than 2 inches (thus allowing the design of a satisfactory joint that does not require terminal anchorages). The charts may also be used for estimating transverse and longitudinal free movements; they can even be used for other concrete pavement types.

5.3.2 Project Evaluation Procedure

This implementation phase seeks to quantify the problem so that the designer may provide a design detail for the plans. The steps are as follows:

(1) Once a specific subbase type has been selected, eight to ten cores are taken from a similar in-situ subbase from 4-inch-diameter samples prepared. For the latter case, the samples should be cored 28 plus days.
(2) Perform splitting tensile tests on each sample and obtain a mean value.
(3) Estimate the mean friction force (K) using the best available equation—i.e., that developed by Wimsatt et al (Ref 16):

$$K = 0.0431 \times 10^{(0.0203St)}$$

where: K = mean friction force, psi, and
St = tensile strength of the specimen, psi.

(4) Estimate the annual temperature variation and concrete thermal coefficient for the pavement thickness to be used. Also select the placement season.
(5) Estimate the joint movement (ΔX) using Equation 5.4.
(6) Select a joint system using the estimated annual joint movement as follows:

(a) If the annual movement is 2 inches or less, a conventional terminal expansion joint should be developed.
(b) If the annual movement is greater than 2 inches, the designer should consider whether the system ought to be restrained by terminal anchorages or by other techniques.

CHAPTER 6. CONCLUSIONS AND RECOMMENDATIONS

6.1 CONCLUSIONS

The general objective of this study was accomplished by developing a procedure that permits the designer to estimate the annual terminal movement as described in Section 5.3. The following specific conclusions were drawn from the analyses and from the results of this study; they are presented in terms of the computer program, field data, and the computational analysis.

PSCP2 computer program:

1. The relationship among factors affecting terminal movement is complex, and the size of the terminal movement depends on whether sliding occurs. Interpreting the field data to determine whether sliding occurs is difficult.
2. The PSCP2 computer program, given proper concrete pavement and subbase data input, can predict free end movement in CRCP.
3. This study shows that the maximum length of CRCP moving is 1,250 feet. The movements measured in the field do not exceed the value of the maximum end movement obtained for each case in this study.

Field data:

1. Movement in the transverse and in the longitudinal directions of CRCP shows similar trends, with transverse movement values being the lesser of the two.
2. In the field, the friction force between CRCP and the subbase is greater than that obtained from the laboratory test.

Computational analysis:

1. Terminal movement is directly related to slab length until the greatest slab length is exceeded. When the greatest slab length is exceeded, the movement is invariant. The value of the greatest slab length varies with environmental conditions.
2. CRC limestone aggregate pavement has approximately two-thirds the end movement of CRC siliceous river gravel aggregate pavement.
3. Thicker CRCP produces more linear end movement.
4. For typical Texas temperature conditions, CRCP winter placement generates approximately 25 percent less end movement than summer placement.
5. Friction force is a significant factor affecting the end movement of CRCP.

6.2 RECOMMENDATIONS FOR PREDICTING END MOVEMENT

The following steps are recommended when using the PSCP2 computer program to predict the free end movement of CRCP.

For correct estimations, the reader should refer to either Figure 5.1 for CRCP or the charts in Appendix A and Appendix B.

1. Figure 5.1 is illustrative of CRCP. The total seasonal temperature change is needed for any computations derived from Figure 5.1.
2. The slab length listed in the charts in Appendix A and Appendix B is the total length of the slab, which is to be used for predicting end movement.
3. The estimations listed in the charts are the movements that occur at one end of the slabs.

For unusual conditions and for more exact estimation, the PSCP2 program should be applied with the following in mind:

1. A proper number of elements should be used, especially when the slab is long. The recommended element length is not more than 15 feet—i.e., 100 elements for a 1,500-foot slab.
2. When a subbase with a higher coefficient of friction is analyzed, more elements should be selected.

3. If the PSCP2 computer program is used to predict the free end movement, then the input item of the ultimate shrinkage strain of the concrete should be zero.
4. If the PSCP2 computer program is used to predict the joint opening, the proper value of the ultimate shrinkage strain of the concrete should be input.

6.3 RECOMMENDATIONS FOR FUTURE STUDY

Areas for future study include the following:

1. More study of the friction resistance between CRCP and the subbase should be conducted in the field, since friction resistance is an important factor affecting the terminal movement of CRCP.
2. More measurements need to be taken of CRCP's constructed over different subbases. These measurements should also include CRCP's of different thicknesses, placement seasons, and aggregate types to obtain more field data on terminal movement.
3. The effects of traffic (wheel load stress) should be incorporated in future studies.
4. A long-term study of terminal movement provisions should be conducted to evaluate the effect of each method.
5. More end movement data should be collected from CRC pavements with terminal anchorage systems to assess the influence of the anchorage system on end movement.

REFERENCES

1. McCullough, B. Frank, "A Field Survey and Exploratory Excavation of Terminal Anchorage Failures on Jointed Concrete Pavement," Research Report 39-1, Texas Highway Department, March 1965.

2. McCullough, B. Frank, and T. F. Sewell, "Parameters Influencing Terminal Movement on Continuously Reinforced Concrete Pavement," Research Report 39-2, Texas Highway Department, August 1964.

3. McCullough, B. Frank, and Fred Herber, "A Report on Continuity between Continuously Reinforced Concrete Pavement and a Continuous Slab Bridge," Research Report 39-3, Texas Highway Department, August 1966.

4. McCullough, B. Frank, "An Evaluation of Terminal Anchorage Installations on Rigid Pavements," Research Report 39-4, Texas Highway Department, September 1966.

5. "Design of Terminals for Rigid Pavements to Control End Movements: State of the Art," Rigid Pavement Design Committee, TRB, 1977.

6. "A Design Procedure for Continuously Reinforced Concrete Pavements for Highway," ACI Committee 325, Subcommittee VII, ACI Journal, June 1972.

7. Aslam, Mohammad F., C. L. Saraf, Ramon L. Carrasquillo, and B. Frank McCullough, "Design Recommendations for Steel Reinforcement of CRCP," Research Report 422-2, Center for Transportation Research, The University of Texas at Austin, November 1987.

8. "Design of Continuously Reinforced Concrete for Highways," ARBP, Highway and Transportation Committee, 1981.

9. Suh, Young-Chan, "Correlation between K- and J-Types of Thermocouples," Tech Memo 1244-9, Center for Transportation Research, The University of Texas at Austin, February 1990.

10. Weissmann, Angela Jannini, and Kenneth Hankins, "A Statewide Diagnostic Survey on Continuously Reinforced Concrete Pavements in Texas," Research Report 472-5, Center for Transportation Research, The University of Texas at Austin, August 1989.

11. Diaz, Alberto Mendoza, Ned H. Burns, and B. Frank McCullough, "Behavior of Long Prestressed Pavement Slabs and Design Methodology," Research Report 401-3, Center for Transportation Research, The University of Texas at Austin, September 1986.

12. Tena-Colunga, José Antonio, B. Frank McCullough, and Ned H. Burns, "Analysis of Curling Movements and Calibration of PCP Program," Research Report 556-3, Center for Transportation Research, The University of Texas at Austin, August 1989.

13. Yoder, E. J., and M. W. Witczak, *Principles of Pavement Design*, Second Edition, John Wiley and Sons, Inc., New York, 1975.

14. Rivero-Vallejo, Felipe, and B. Frank McCullough, "Drying Shrinkage and Temperature Drop Stresses in Jointed Reinforced Concrete Pavement," Research Report 177-1, Center for Transportation Research, The University of Texas at Austin, August 1975.

15. Wu, Wan-Yi, "Prediction of End Movement in CRCP Using Computer Program JRCP5," Tech Memo 1244-53, Center for Transportation Research, The University of Texas at Austin, December 1990.

16. Wimsatt, Andrew W., B. Frank McCullough, and Ned H. Burns, "Methods of Analyzing and Factors Influencing Frictional Effects of Subbases," Research Report 459-2F, Center for Transportation Research, The University of Texas at Austin, November 1987.

17. Chiang, Chypin, B. Frank McCullough, and W. R. Hudson, "A Sensitivity Analysis of Continuously Reinforced Concrete Pavement Model CRCP-1 for Highways," Research Report 177-2, Center for Transportation Research, The University of Texas at Austin, August 1975.

18. Mandel, Elliott, José Tena-Colunga, and Kenneth Hankins, "Performance Tests on a Prestressed Concrete Pavement–Presentation of Data," Research Report 556-1, Center for Transportation Research, The University of Texas at Austin, November 1989.

19. Suh, Young-Chan, "Slab Temperature Study," Tech Memo 422-68, Center for Transportation Research, The University of Texas at Austin, August 1989.

APPENDIX A. GRAPHS OF END AND SEASONAL MOVEMENT IN RELATION TO SLAB LENGTH

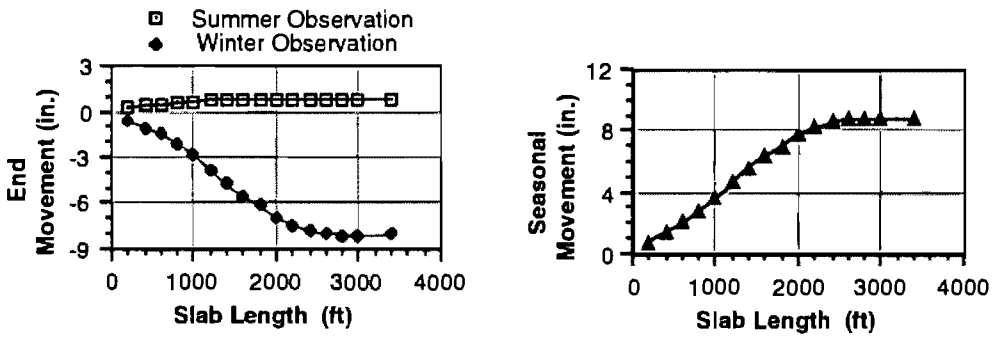

Figure A.1 **End and seasonal movements in relation to slab length for 12-inch-thick SRG aggregate slab placed in the summer over a subbase with a 1.0 psi friction force**

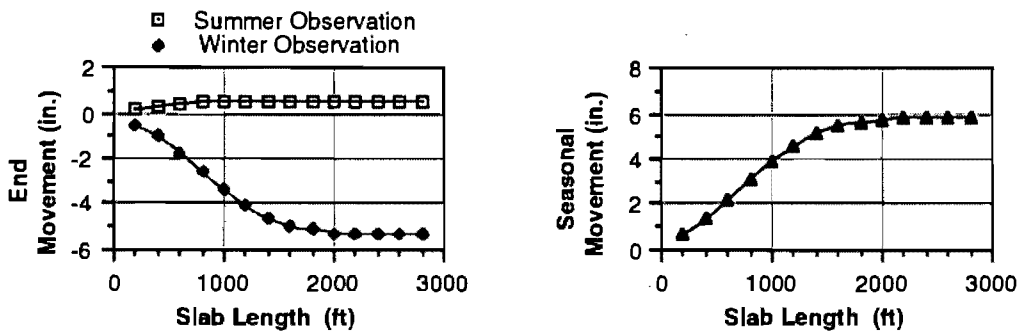

Figure A.2 **End and seasonal movements in relation to slab length for 8-inch-thick SRG aggregate slab placed in the summer over a subbase with a 1.0 psi friction force**

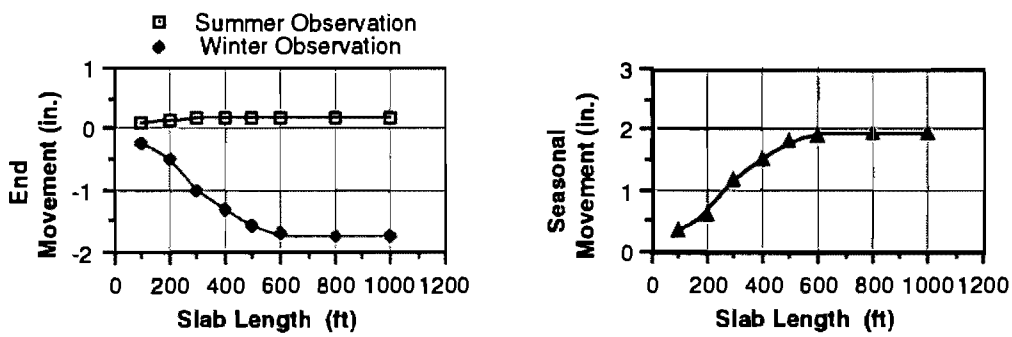

Figure A.3 **End and seasonal movements in relation to slab length for 12-inch-thick SRG aggregate slab placed in the summer over a subbase with a 4.6 psi friction force**

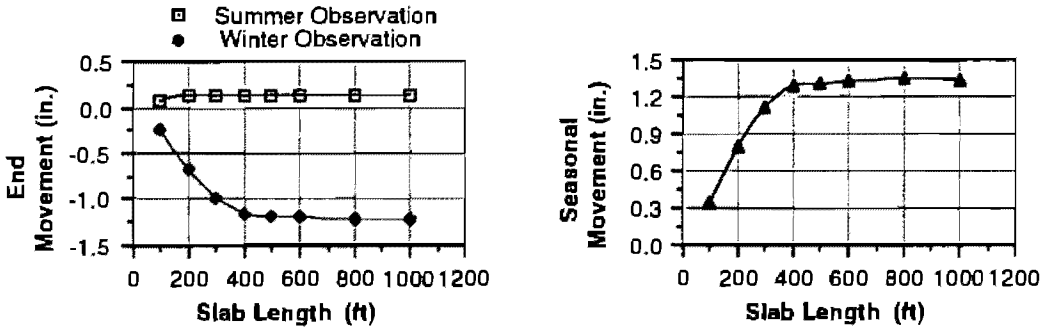

Figure A.4 End and seasonal movements in relation to slab length for 8-inch-thick SRG aggregate slab placed in the summer over a subbase with a 4.6 psi friction force

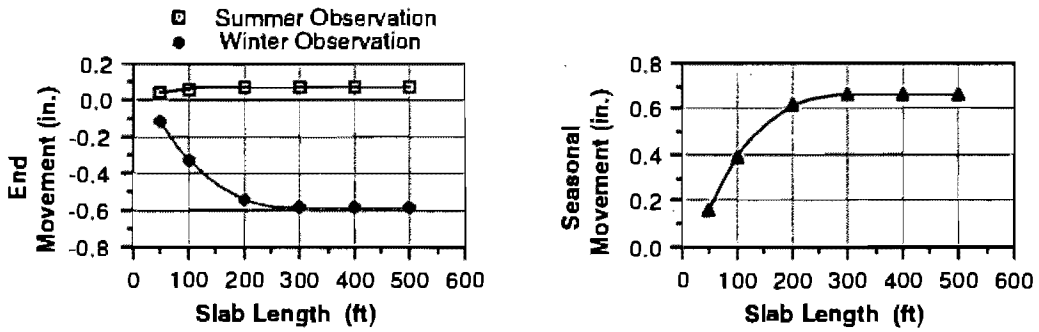

Figure A.5 End and seasonal movements in relation to slab length for 12-inch-thick SRG aggregate slab placed in the summer over a subbase with a 15 psi friction force

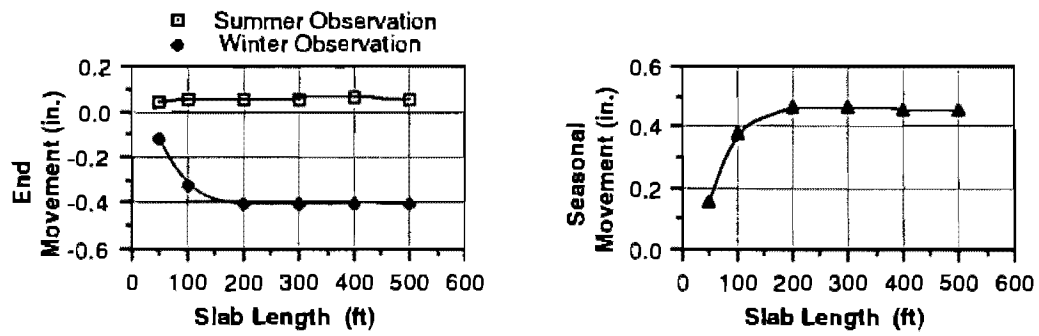

Figure A.6 End and seasonal movements in relation to slab length for 8-inch-thick SRG aggregate slab placed in the summer over a subbase with a 15 psi friction force

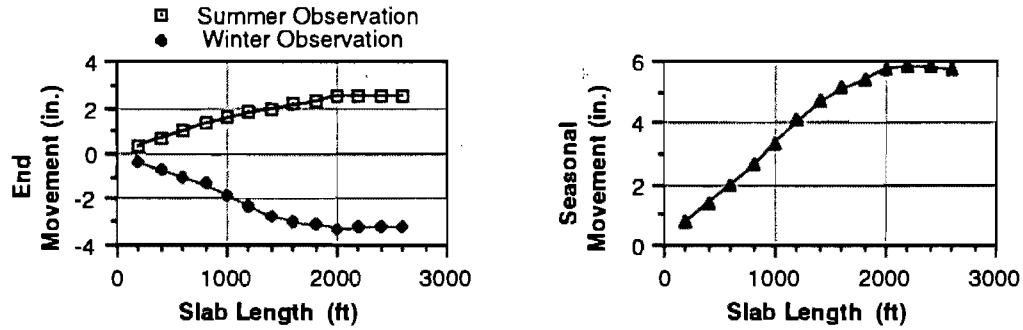

Figure A.7 **End and seasonal movements in relation to slab length for 12-inch-thick SRG aggregate slab placed in the winter over a subbase with a 1.0 psi friction force**

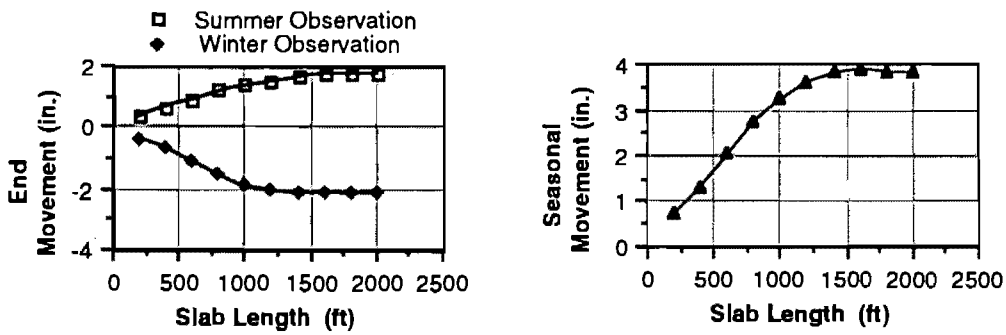

Figure A.8 **End and seasonal movements in relation to slab length for 8-inch-thick SRG aggregate slab placed in the winter over a subbase with a 1.0 psi friction force**

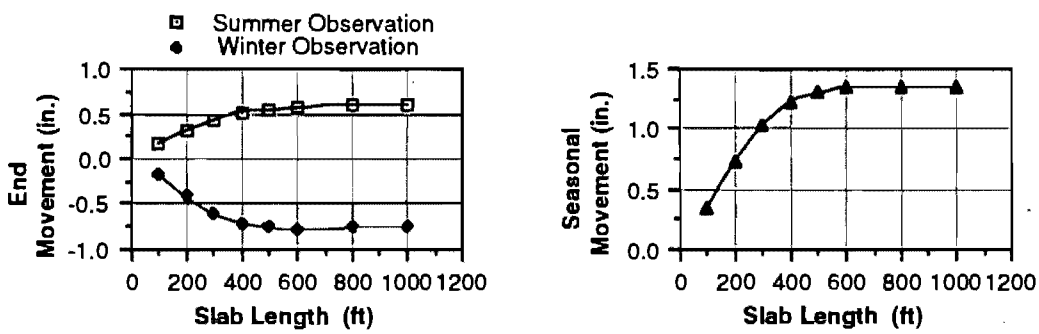

Figure A.9 **End and seasonal movements in relation to slab length for 12-inch-thick SRG aggregate slab placed in the winter over a subbase with a 4.6 psi friction force**

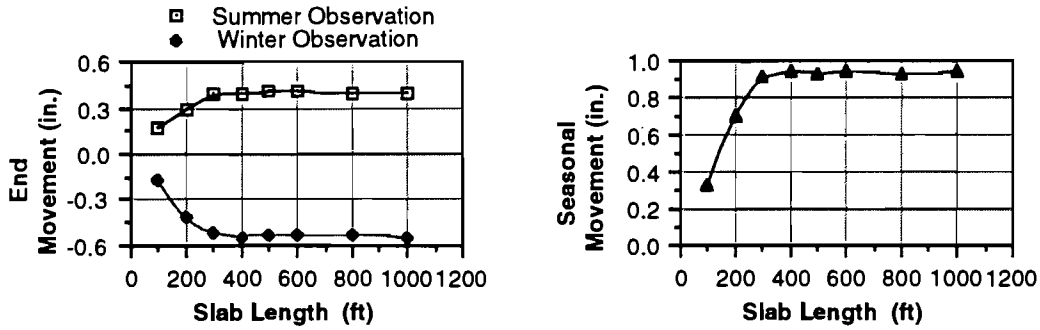

Figure A.10 End and seasonal movements in relation to slab length for 8-inch-thick SRG aggregate slab placed in the winter over a subbase with a 4.6 psi friction force

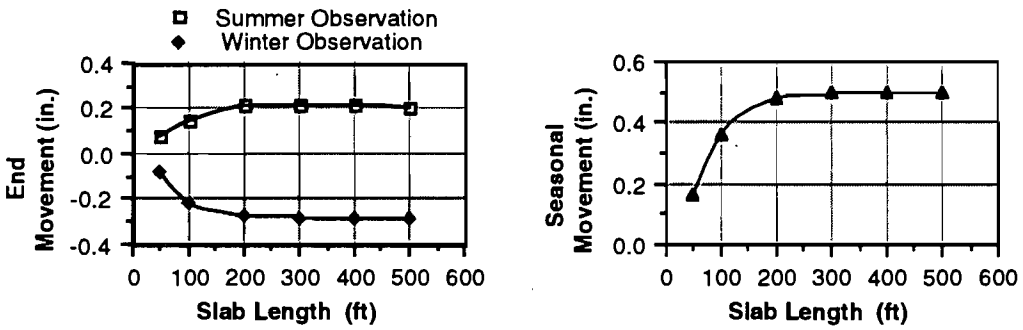

Figure A.11 End and seasonal movements in relation to slab length for 12-inch-thick SRG aggregate slab placed in the winter over a subbase with a 15 psi friction force

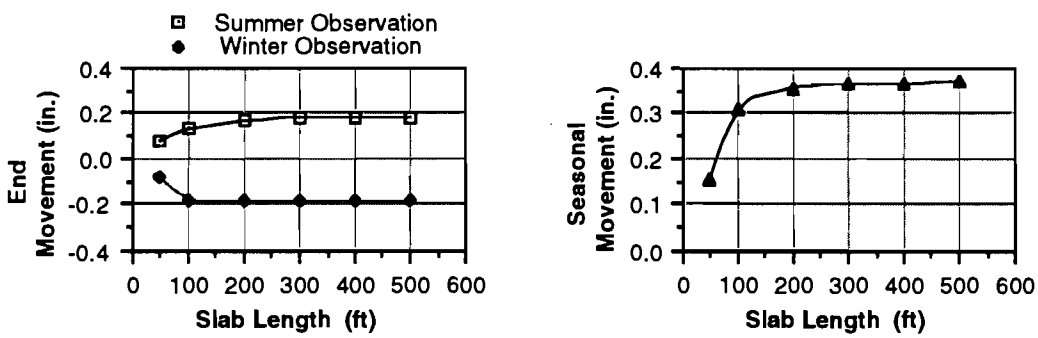

Figure A.12 End and seasonal movements in relation to slab length for 8-inch-thick SRG aggregate slab placed in the winter over a subbase with a 15 psi friction force

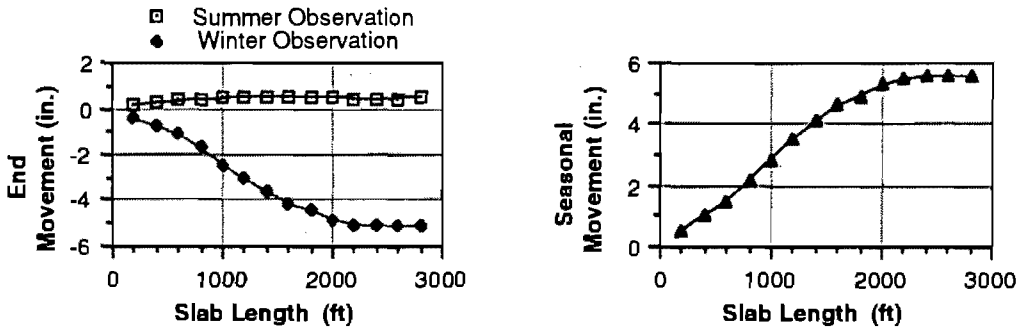

Figure A.13 End and seasonal movements in relation to slab length for 12-inch-thick LS aggregate slab placed in the summer over a subbase with a 1.0 psi friction force

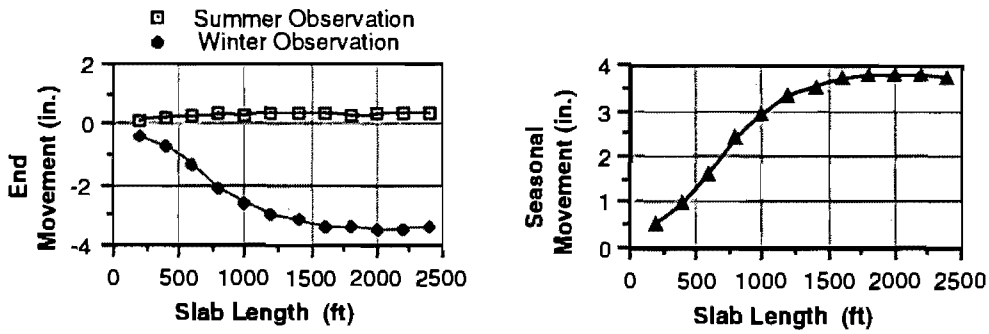

Figure A.14 End and seasonal movements in relation to slab length for 8-inch-thick LS aggregate slab placed in the summer over a subbase with a 1.0 psi friction force

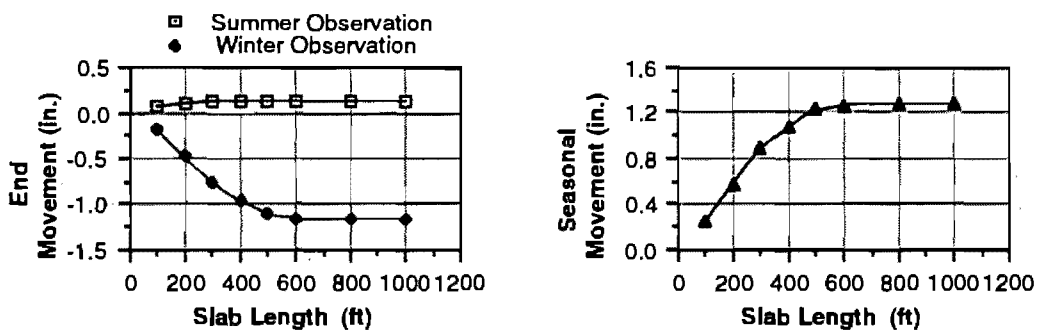

Figure A.15 End and seasonal movements in relation to slab length for 12-inch-thick LS aggregate slab placed in the summer over a subbase with a 4.6 psi friction force

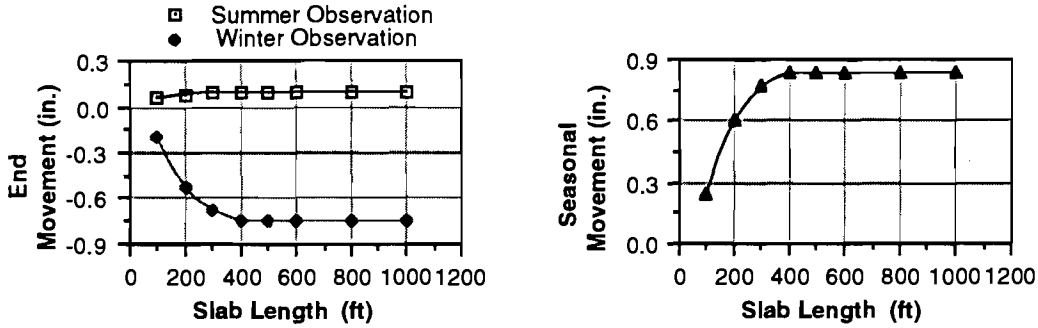

Figure A.16 End and seasonal movements in relation to slab length for 8-inch-thick LS aggregate slab placed in the summer over a subbase with a 4.6 psi friction force

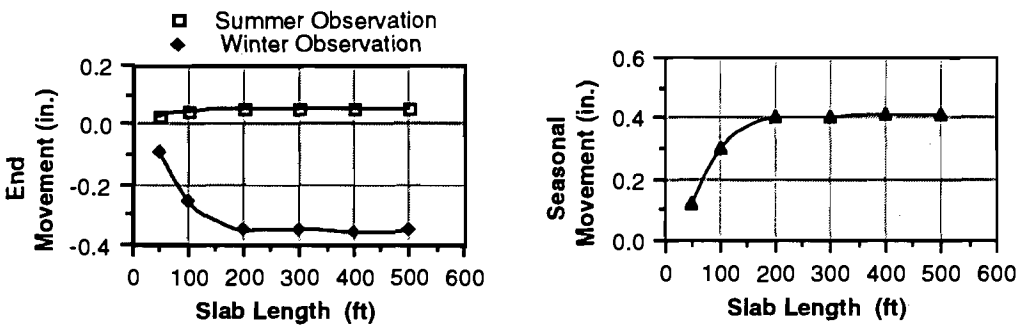

Figure A.17 End and seasonal movements in relation to slab length for 12-inch-thick LS aggregate slab placed in the summer over a subbase with a 15 psi friction force

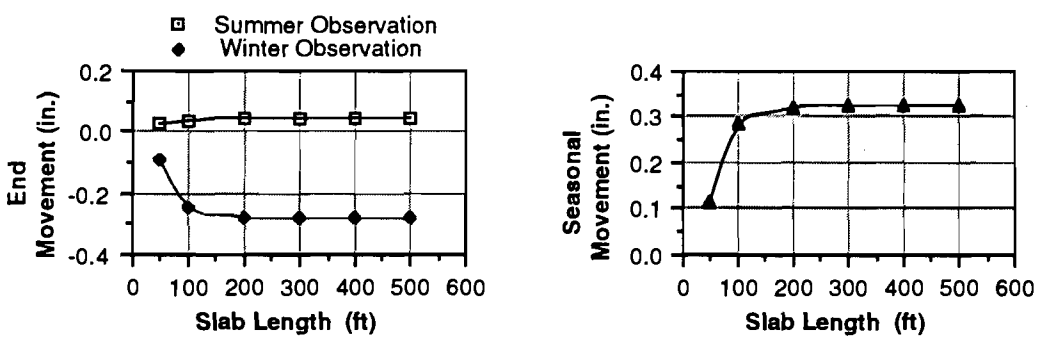

Figure A.18 End and seasonal movements in relation to slab length for 8-inch-thick LS aggregate slab placed in the summer over a subbase with a 15 psi friction force

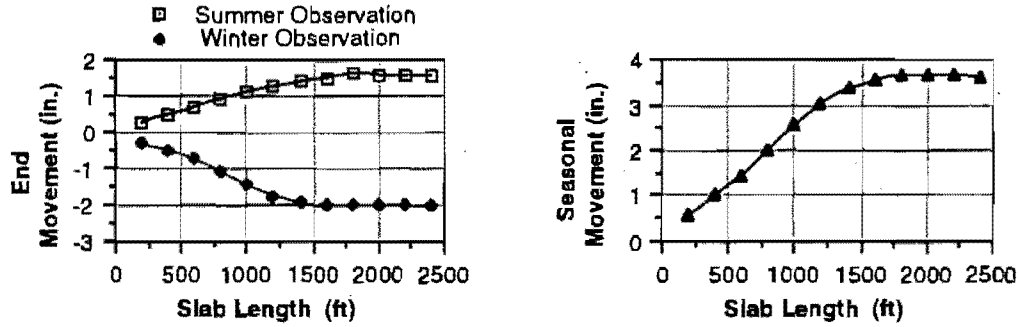

Figure A.19 End and seasonal movements in relation to slab length for 12-inch-thick LS aggregate slab placed in the winter over a subbase with a 1.0 psi friction force

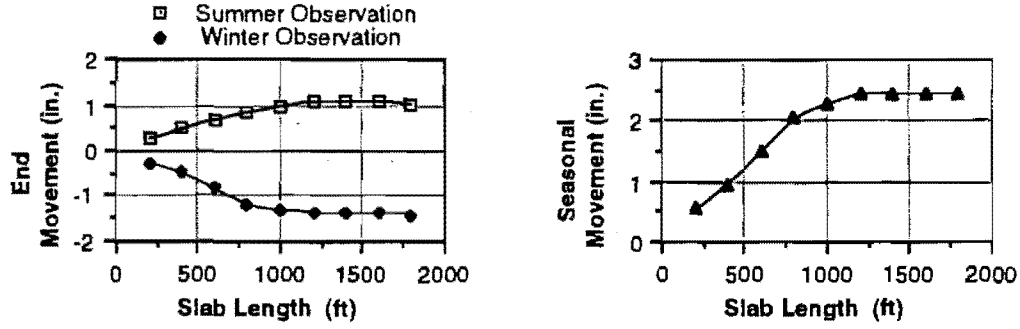

Figure A.20 End and seasonal movements in relation to slab length for 8-inch-thick LS aggregate slab placed in the winter over a subbase with a 1.0 psi friction force

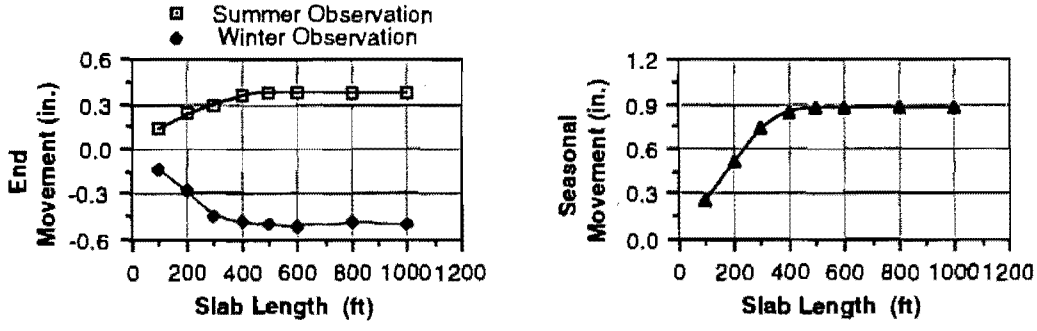

Figure A.21 End and seasonal movements in relation to slab length for 12-inch-thick LS aggregate slab placed in the winter over a subbase with a 4.6 psi friction force

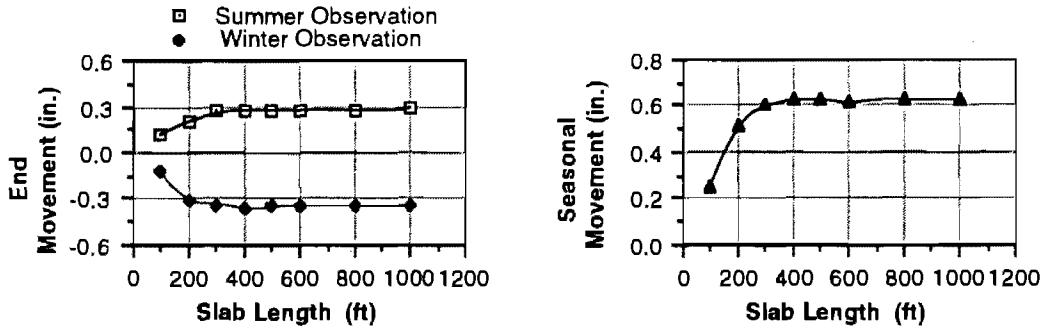

Figure A.22 End and seasonal movements in relation to slab length for 8-inch-thick LS aggregate slab placed in the winter over a subbase with a 4.6 psi friction force

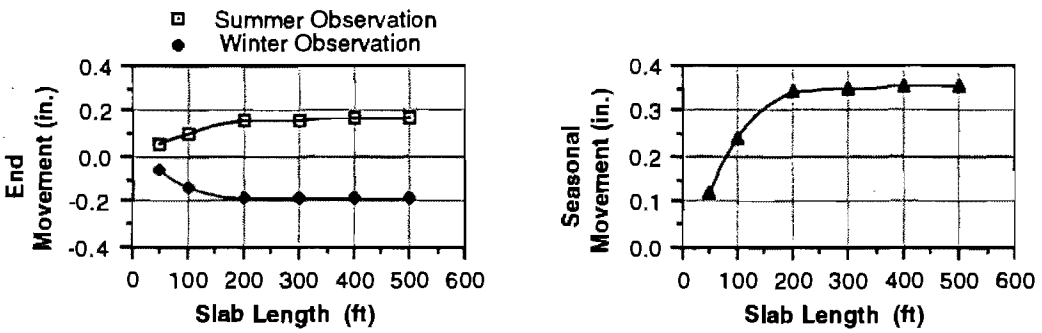

Figure A.23 End and seasonal movements in relation to slab length for 12-inch-thick LS aggregate slab placed in the winter over a subbase with a 15 psi friction force

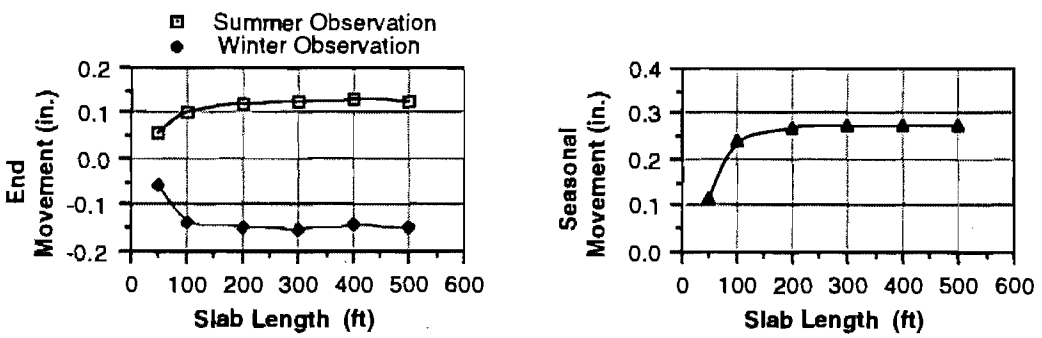

Figure A.24 End and seasonal movements in relation to slab length for 8-inch-thick LS aggregate slab placed in the winter over a subbase with a 15 psi friction force

APPENDIX B. GRAPHS OF RATE OF MOVEMENT IN RELATION TO SLAB LENGTH

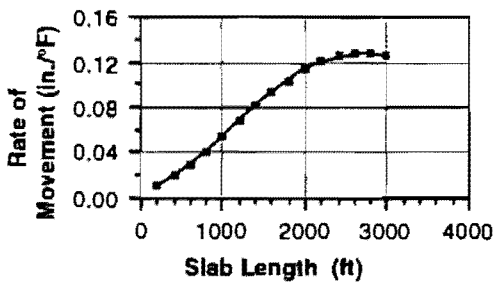

Figure B.1 Rate of movement in relation to slab length for 12-inch-thick SRG aggregate slab placed in the summer over a subbase with a 1.0 psi friction force

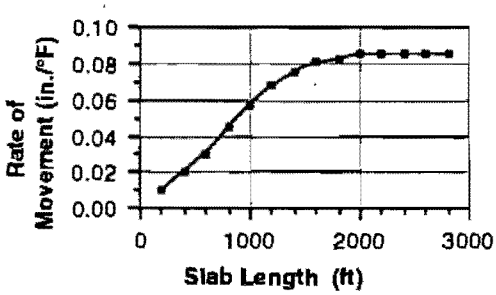

Figure B.2 Rate of movement in relation to slab length for 8-inch-thick SRG aggregate slab placed in the summer over a subbase with a 1.0 psi friction force

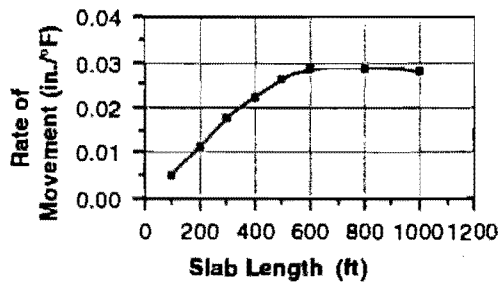

Figure B.3 Rate of movement in relation to slab length for 12-inch-thick SRG aggregate slab placed in the summer over a subbase with a 4.6 psi friction force

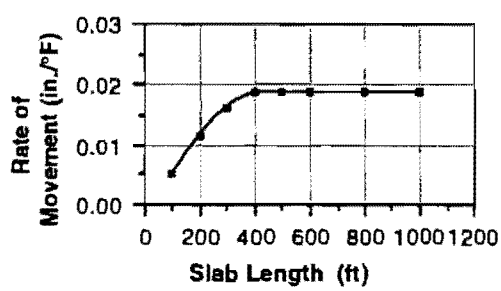

Figure B.4 Rate of movement in relation to slab length for 8-inch-thick SRG aggregate slab placed in the summer over a subbase with a 4.6 psi friction force

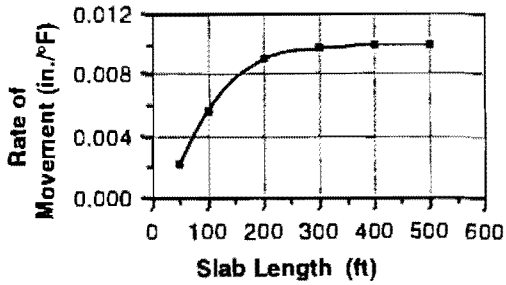

Figure B.5 Rate of movement in relation to slab length for 12-inch-thick SRG aggregate slab placed in the summer over a subbase with a 15 psi friction force

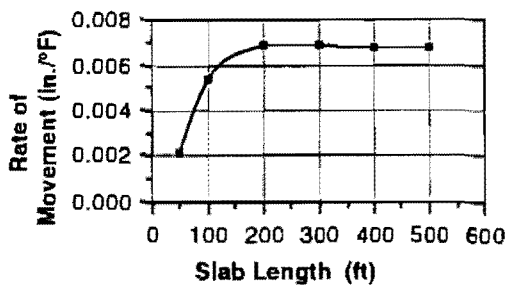

Figure B.6 Rate of movement in relation to slab length for 8-inch-thick SRG aggregate slab placed in the summer over a subbase with a 15 psi friction force

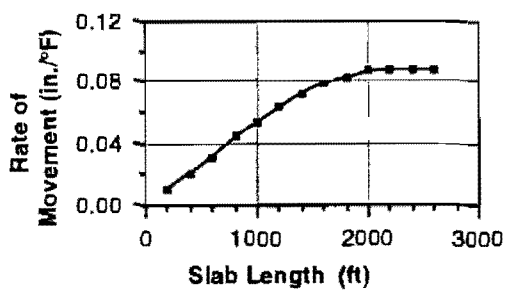

Figure B.7 Rate of movement in relation to slab length for 12-inch-thick SRG aggregate slab placed in the winter over a subbase with a 1.0 psi friction force

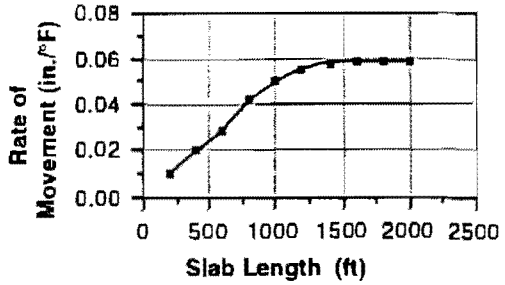

Figure B.8 Rate of movement in relation to slab length for 8-inch-thick SRG aggregate slab placed in the winter over a subbase with a 1.0 psi friction force

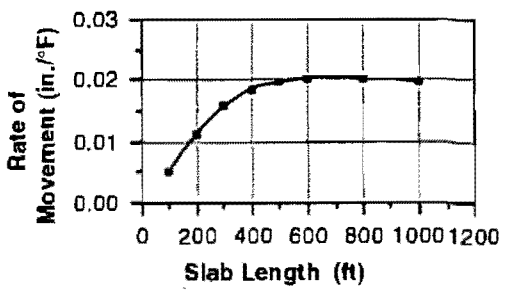

Figure B.9 Rate of movement in relation to slab length for 12-inch-thick SRG aggregate slab placed in the winter over a subbase with a 4.6 psi friction force

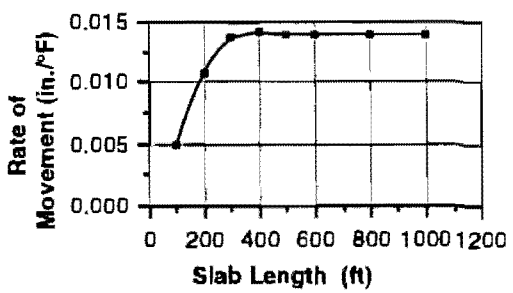

Figure B.10 Rate of movement in relation to slab length for 8-inch-thick SRG aggregate slab placed in the winter over a subbase with a 4.6 psi friction force

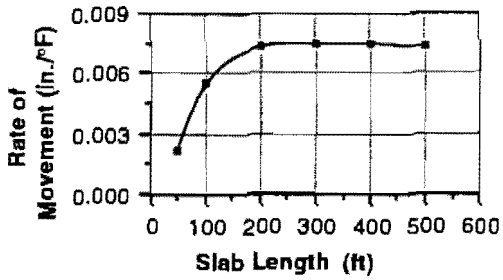

Figure B.11 Rate of movement in relation to slab length for 12-inch-thick SRG aggregate slab placed in the winter over a subbase with a 15 psi friction force

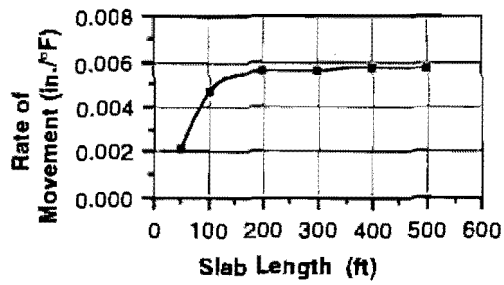

Figure B.12 Rate of movement in relation to slab length for 8-inch-thick SRG aggregate slab placed in the winter over a subbase with a 15 psi friction force

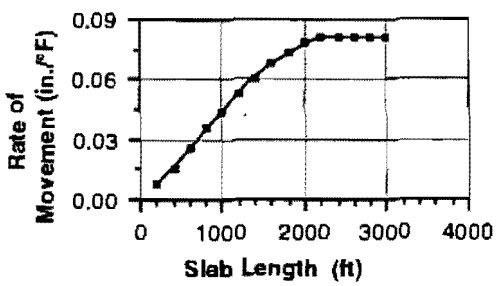

Figure B.13 Rate of movement in relation to slab length for 12-inch-thick LS aggregate slab placed in the summer over a subbase with a 1.0 psi friction force

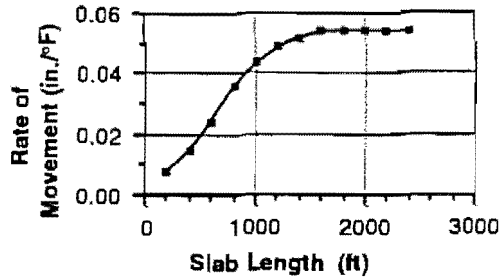

Figure B.14 Rate of movement in relation to slab length for 8-inch-thick LS aggregate slab placed in the summer over a subbase with a 1.0 psi friction force

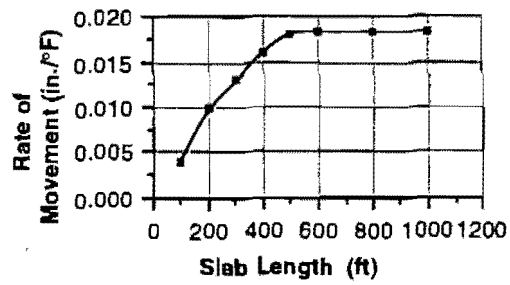

Figure B.15 Rate of movement in relation to slab length for 12-inch-thick LS aggregate slab placed in the summer over a subbase with a 4.6 psi friction force

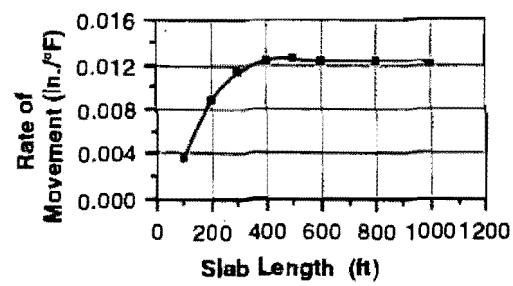

Figure B.16 Rate of movement in relation to slab length for 8-inch-thick LS aggregate slab placed in the summer over a subbase with a 4.6 psi friction force

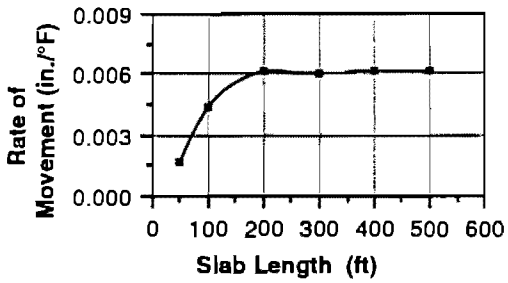

Figure B.17 Rate of movement in relation to slab length for 12-inch-thick LS aggregate slab placed in the summer over a subbase with a 15 psi friction force

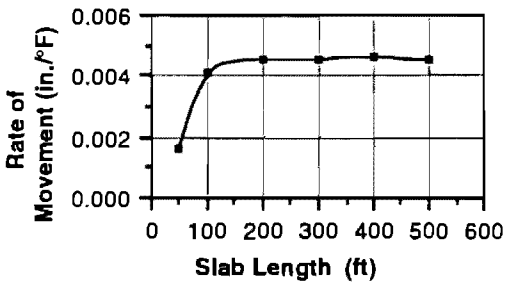

Figure B.18 Rate of movement in relation to slab length for 8-inch-thick LS aggregate slab placed in the summer over a subbase with a 15 psi friction force

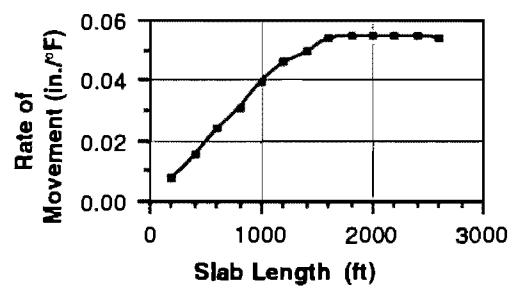

Figure B.19 Rate of movement in relation to slab length for 12-inch-thick LS aggregate slab placed in the winter over a subbase with a 1.0 psi friction force

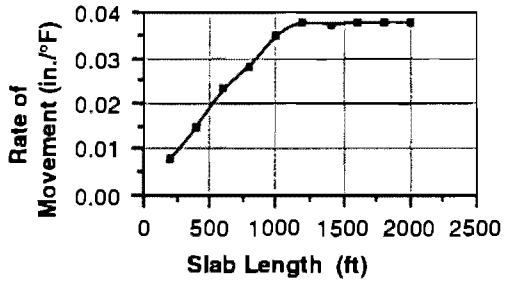

Figure B.20 Rate of movement in relation to slab length for 8-inch-thick LS aggregate slab placed in the winter over a subbase with a 1.0 psi friction force

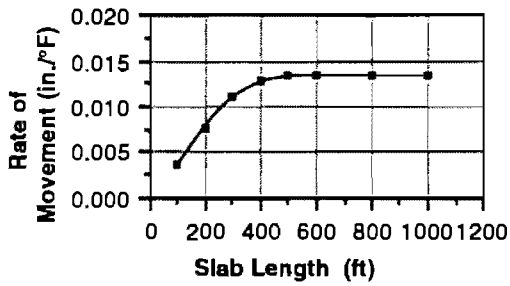

Figure B.21 Rate of movement in relation to slab length for 12-inch-thick LS aggregate slab placed in the winter over a subbase with a 4.6 psi friction force

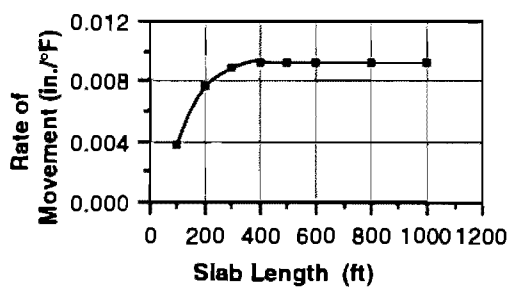

Figure B.22 Rate of movement in relation to slab length for 8-inch-thick LS aggregate slab placed in the winter over a subbase with a 4.6 psi friction force

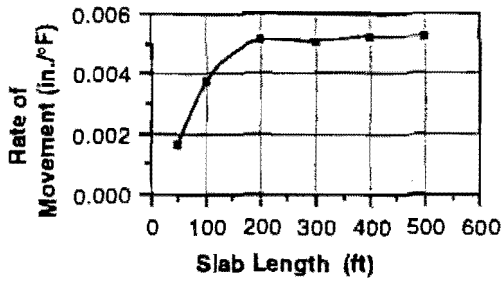

Figure B.23 Rate of movement in relation to slab length for 12-inch-thick LS aggregate slab placed in the winter over a subbase with a 15 psi friction force

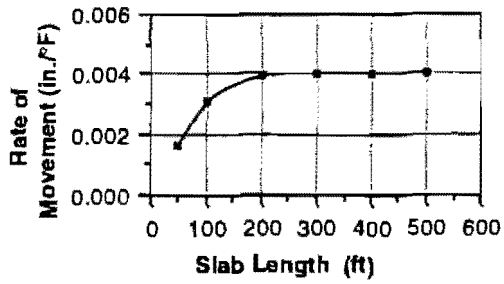

Figure B.24 Rate of movement in relation to slab length for 8-inch-thick LS aggregate slab placed in the winter over a subbase with a 15 psi friction force

APPENDIX C. DATA FROM MEASUREMENT TAKEN ON SH 225 IN HOUSTON

APPENDIX C Measurement Results at SH 225 in Houston									
Time	Temperature		Gauge Plug Reading						
	Air	Concrete	A	B	C	D	E	F	G
4/8/91									
4:40 PM	84.8	86.5	9.9919	10.0087	10.0034	10.0165			
6:40 PM	81.6	82.6	9.9957	10.0173	10.0077	10.0177			
7:15 PM	82	80.4	9.9971	10.0184	10.0066	10.0179			
4/9/91									
7:25 AM	72.8	71.8	10.0132	10.0467	10.0086	10.0216			
8:55 AM	75	72.5	10.0128	10.0459	10.0086	10.0204			
10:30 AM	78.4	74.1	10.0091	10.0402	10.0056	10.018	10.0227		
11:00 AM	79.8	75.1	10.0059	10.0389	10.0074	10.0178	10.0206	9.9901	9.9831
12:20 PM	84	78.6	9.9985	10.029	10.0053	10.0156	10.0113	9.9662	9.9573
1:20 PM	83.8	79.7	9.9927	10.0212	10.0049	10.0147	10.0054	9.9302	9.9213
2:20 PM	81.6	78.9	9.9944	10.0231	10.0064	10.0164	10.0035	9.9258	9.9131
3:20 PM	89.6	82.3	9.9871	10.0119	10.0039	10.0132	9.9955	9.8955	9.8707
4:20 PM	88.8	85.8	9.985	10.0087	10.0035	10.0128	9.9899	9.8644	9.8423
5:20 PM	86.4	84.1	9.9881	10.0114	10.0054	10.0148	9.988	9.8586	9.8329
6:30 PM	84.6	82.7	9.9918	10.0163	10.0068	10.0166	9.9887	9.8555	9.8313
4/10/91									
6:20 AM	70.4	71.3	10.0148	10.0469	10.0123	10.0226	10.0208	9.9804	9.9759
7:40 AM	69.2	70.4	10.0162	10.0492	10.011	10.0229	10.0188	9.9932	9.99
8:30 AM	71	71.0	10.0156	10.0484	10.0105	10.0191	10.0187	9.9956	9.9921
9:30 AM	72.4	71.9	10.0138	10.0461	10.0089	10.0206	10.0155	9.9946	9.9897
10:30 AM	77.6	75.6	10.0029	10.0346	10.0063	10.0163	10.0108	9.9803	9.9734

APPENDIX D. GRAPHS OF GAUGE PLUG READINGS AND SLAB TEMPERATURES AT SH 225 IN HOUSTON

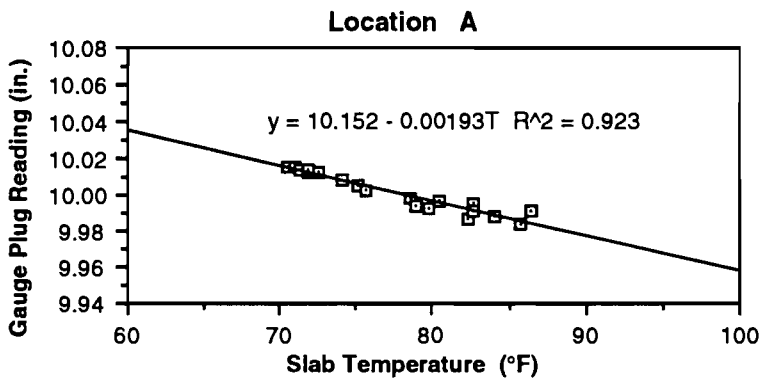

Figure D.1 Gauge plug reading and slab temperature at Location A

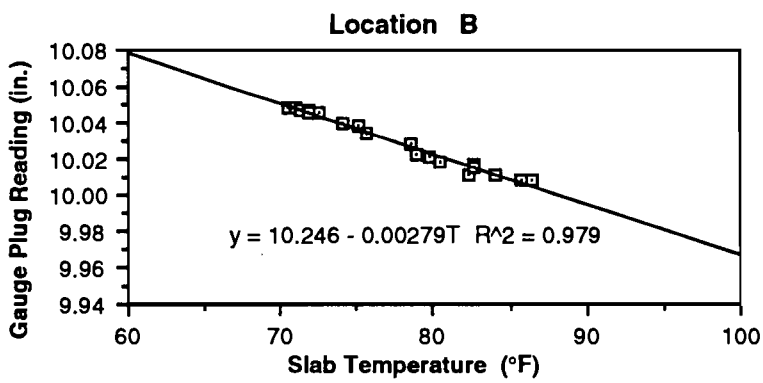

Figure D.2 Gauge plug reading and slab temperature at Location B

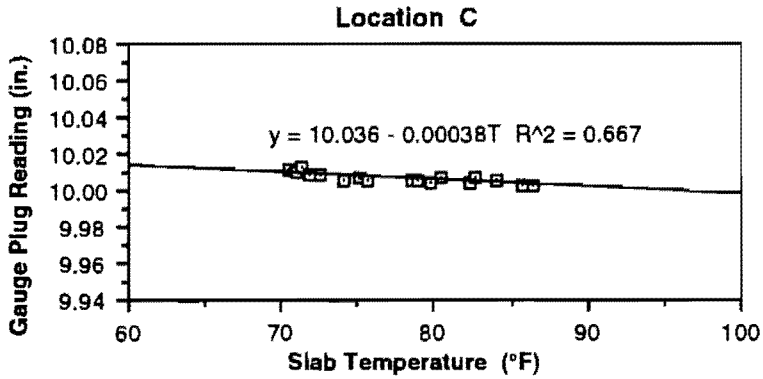

Figure D.3 Gauge plug reading and slab temperature at Location C

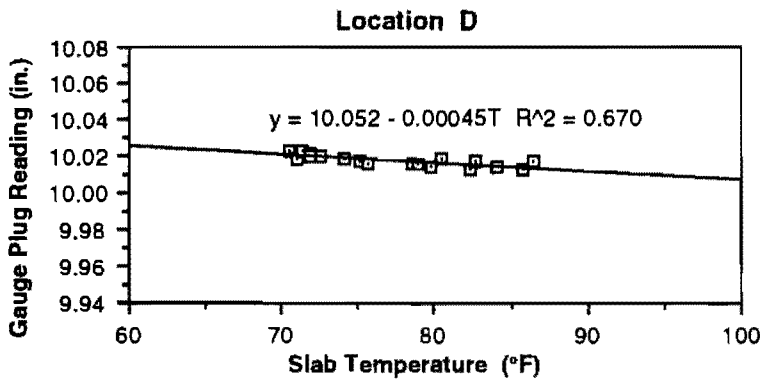

Figure D.4 Gauge plug reading and slab temperature at Location D

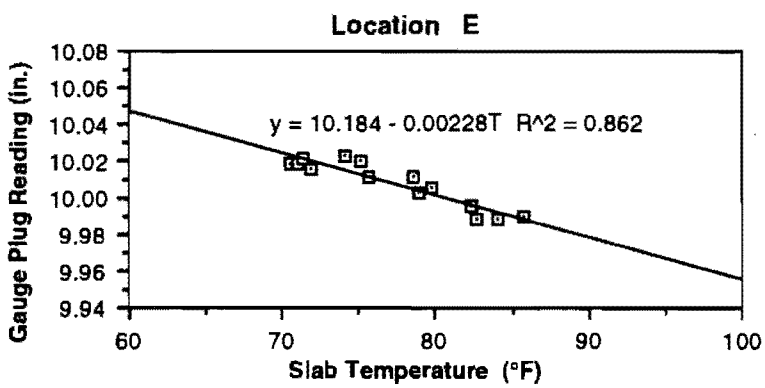

Figure D.5 Gauge plug reading and slab temperature at Location E

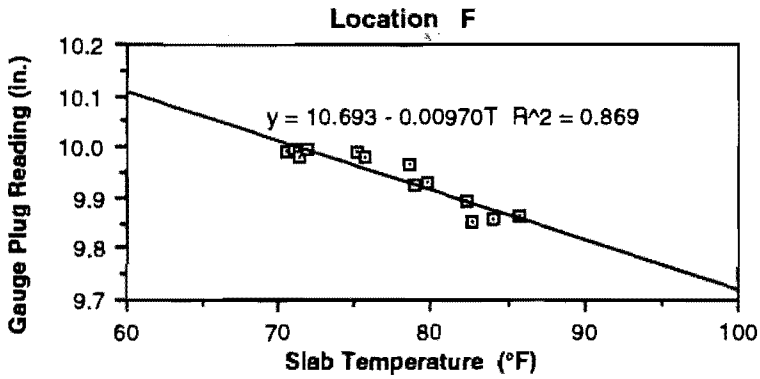

Figure D.6 Gauge plug reading and slab temperature at Location F

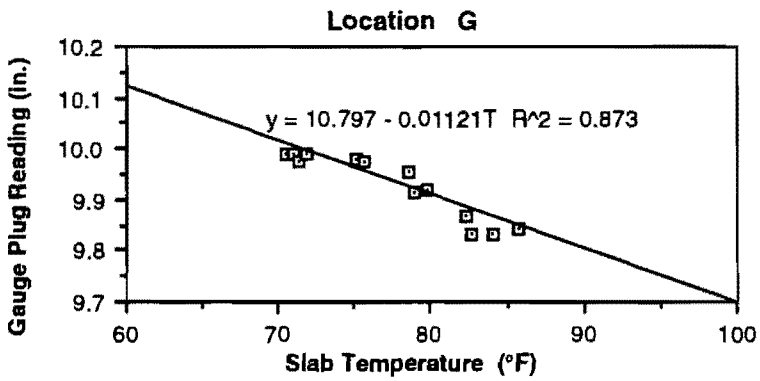

Figure D.7 Gauge plug reading and slab temperature at Location G